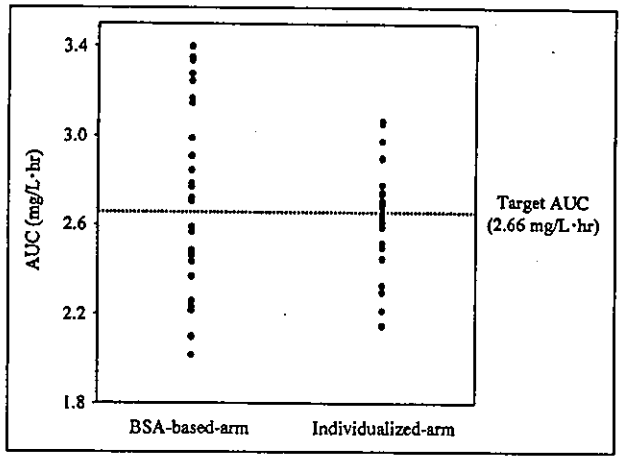

Fig 3. Comparison of area under the concentration-time curve (AUC) variability between the arms ($P < .01$; F test). BSA, body-surface area.

achieved a partial response in the BSA-based arm and individualized arm, respectively.

DISCUSSION

In oncology practice, the prescribed dose of most anticancer drugs is currently calculated from BSA of individual patients to reduce the interpatient variability of drug exposure. However, PK parameters, such as CL of many anticancer drugs, are not related to BSA.[2,39-43] Although PK parameters of docetaxel are correlated with BSA, individualized dosing based on individual metabolic capacities could further decrease the interpatient variability.[43]

CYP3A4 plays an important role in the metabolism of many drugs, including anticancer agents such as docetaxel, paclitaxel, vinorelbine, and gefitinib. This enzyme exhibits a large interpatient variability in metabolic activity, accounting for the large interpatient PK and PD variability. We have developed a novel method of estimating the interpatient variability of CYP3A4 activity by urinary metabolite of exogenous cortisol. That is, the total amount of 24-hour urinary 6-β-OHF after cortisol administration was highly correlated with docetaxel CL. We conducted a prospective randomized PK and PD study of docetaxel to evaluate whether the application of our method to individualized dosing could decrease PK and PD variability compared with BSA-based dosing.

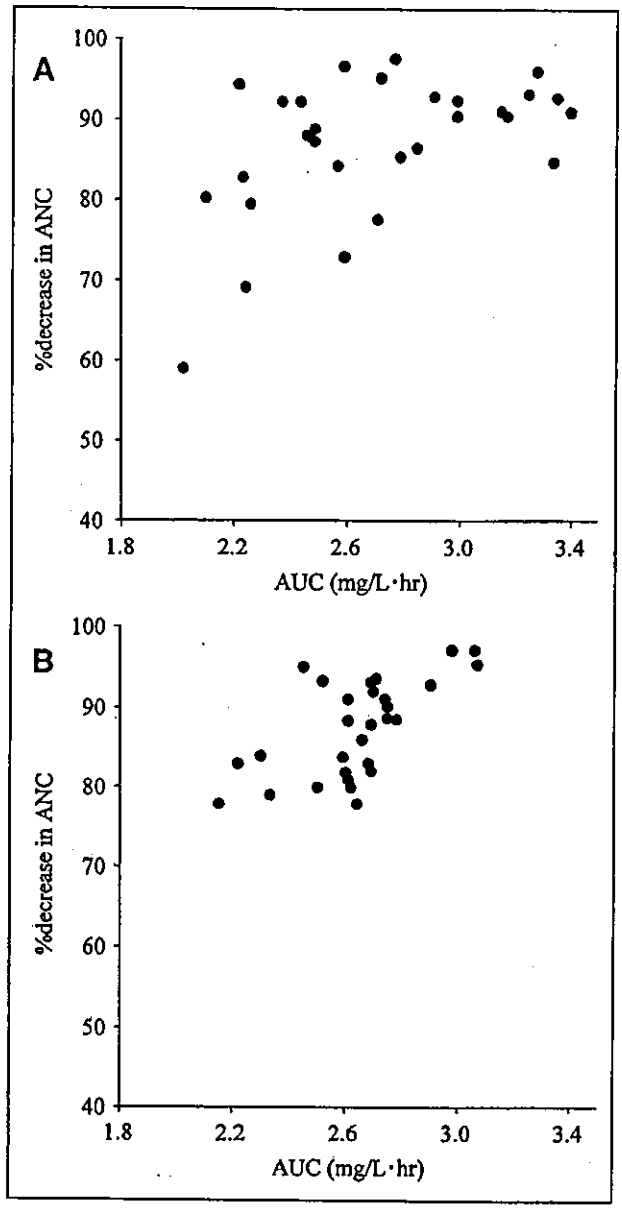

Fig 4. Correlation between area under the concentration-time curve (AUC) and percentage decrease in absolute neutrophil count (ANC) in each arm. (A) body-surface area–based arm; (B) individualized arm.

Table 3. Percentage Decrease in ANC

Parameters	BSA-Based Arm (n = 30)	Individualized Arm (n = 29)
Percentage decrease in ANC, %		
Mean	87.1	87.4
Range	59.0-97.7	78.0-97.2
Median	89.7	88.4
SD	8.7	8.1

Abbreviations: ANC, absolute neutrophil count; BSA, body-surface area; SD, standard deviation.

The study by Hirth et al[28] showed a good correlation between the result of the erythromycin breath test and docetaxel CL, and the study by Goh et al[29] showed a good correlation between the midazolam CL and docetaxel CL. In our study, we prospectively validated the correlation between docetaxel CL and our previously published method using the total amount of urinary 6-β-OHF after

cortisol administration in the individualized arm. As shown in Fig 2, the observed docetaxel CL was well estimated, and the equation for the estimation of docetaxel CL developed in our previous study was found to be reliable and reproducible. The target AUC in the individualized arm was set at 2.66 mg/L · h. This value was the mean value from our previous study, in which 29 patients were treated with 60 mg/m^2 of docetaxel. Individualized doses of docetaxel ranged from 37.4 to 76.4 mg/m^2 and were lower than expected.

The SD of AUC in the individualized arm was about 46.2% smaller than that in the BSA-based arm, a significant difference; this result seems to indicate that the application of our method to individualized dosing can reduce the interpatient PK variability. Assuming that the variability of AUC could be decreased 46.2% by individualized dosing applying our method, overtreatment could be avoided in 14.5% of BSA-dosed patients by using individualized dosing (Fig 5, area A), and undertreatment could be avoided in another 14.5% of these patients (Fig 5, area B). We considered that neutropenia could be decreased with patients in area A by individualized dosing. However, it is unknown whether the therapeutic effect of docetaxel could be improved in the patients in area B by individualized dosing because no significant positive correlation has been found between docetaxel AUC and antitumor response in patients with non–small-cell lung cancer.[43] In this study, seven of 30 (23.3%) and two of 30 (6.7%) patients in the BSA-based arm were included in area A and B, respectively (Figs 3 and 5).

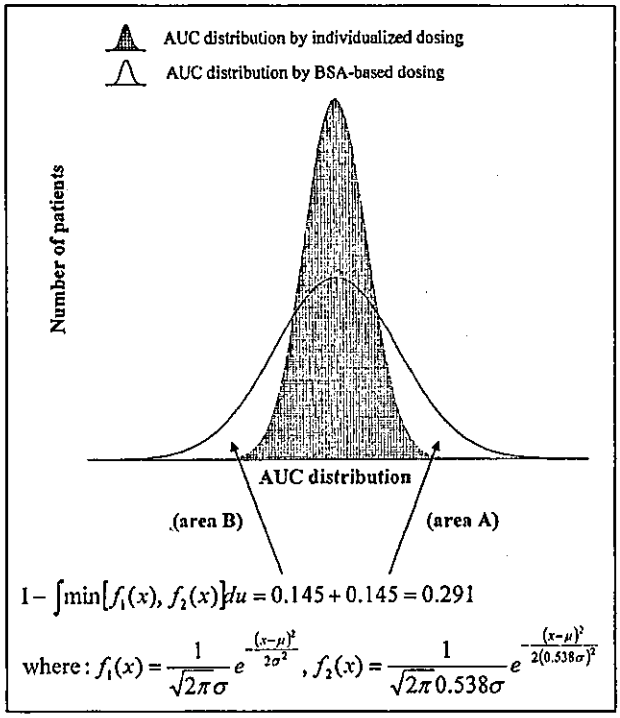

Fig 5. Simulated comparison of area under the concentration-time curve (AUC) distribution between body-surface area (BSA) –based dosing and individualized dosing when the variability of AUC is decreased 46.2% by individualized dosing applied using our method.

As shown in Figure 4, the percentage decrease in ANC was well correlated with AUC in both arms, which was similar to previous reports.[37,43] It was also indicated that the interpatient variability in the percentage decrease in ANC was slightly smaller in the individualized arm than in the BSA-based arm; however, this difference was not significant. The response rates between the two arms were similar. Although the interpatient PK variability could be decreased by individualized dosing in accordance with our method, the interpatient PD variability such as toxicity and the antitumor response could not be decreased. Several reasons could be considered.

With regard to toxicity, the pretreatment characteristics of the patients in this study were highly variable. More than half of the patients in each arm had previously received platinum-based chemotherapy, and more than 30% had received radiotherapy. The laboratory parameters (ie, ALB, AAG, and ALP) were not balanced across the arms, although they were not included in the eligibility criteria (Table 1). These variable pretreatment characteristics and unbalanced laboratory parameters may have influenced the frequency and severity of the hematologic toxicity as well as the pharmacokinetic profiles. The antitumor effect may have been influenced by the intrinsic sensitivity of tumors, the variable pretreatment characteristics, and the imbalance in laboratory parameters. Non–small-cell lung cancer is a chemotherapy-resistant tumor. The response rate for docetaxel ranges from 18% to 38%,[5] and no significant positive correlation between docetaxel AUC and antitumor response has been found. We considered it quite difficult to control the interpatient PD variability by controlling the interpatient PK variability alone. Although we did not observe any outliers in either arm, such as the two outliers with severe toxicity observed in the study by Hirth et al,[28] our method may be more useful for identifying such outliers. If we had not excluded patients with more abnormal liver function or a history of liver disease by the strict eligibility criteria, the results with the two dosing regimens may have been more different, and the interpatient PD variability, such as the percentage decrease in ANC, may have been smaller in the individualized arm than in the BSA-based arm. Furthermore, the primary end point of this study was PK variability, evaluated by the SD of AUC in both arms, and the sample size was significantly underpowered to evaluate whether the application of our method to individualized dosing could decrease PD variability compared with BSA-based dosing.

For the genotypes of CYP3A4, several genetic polymorphisms have been reported (http://www.imm.ki.se/CYPalleles/); however, a clear relationship between genetic polymorphisms and the enzyme activity of CYP3A4 has not been reported. Our phenotype-based

individualized dosing using the total amount of urinary 6-β-OHF after cortisol administration produced good results. However, this method is somewhat complicated, and a simpler method would be of great use. We analyzed the expression of CYP3A4 mRNA in the peripheral-blood mononuclear cells of the 29 patients in the individualized arm. No correlation was observed between the expression level of CYP3A4 mRNA and docetaxel CL or the total amount of urinary 6-β-OHF after cortisol administration (data not shown).

In conclusion, the individualized dosing of docetaxel using the total amount of urinary 6-β-OHF after cortisol administration is useful for decreasing the interpatient PK variability compared with the conventional BSA-based method of dosing. This method may be useful for individualized chemotherapy.

Authors' Disclosures of Potential Conflicts of Interest

The authors indicated no potential conflicts of interest.

REFERENCES

1. Sawyer M, Ratain MJ: Body surface area as a determinant of pharmacokinetics and drug dosing. Invest New Drugs 19:171-177, 2001
2. Gurney H: Dose calculation of anticancer drugs: A review of the current practice and introduction of an alternative. J Clin Oncol 14: 2590-2611, 1996
3. Ratain MJ: Body-surface area as a basis for dosing of anticancer agents: Science, myth, or habit? J Clin Oncol 16:2297-2298, 1998
4. Ringel I, Horwitz SB: Studies with RP 56976 (Taxotere): A semisynthetic analogue of taxol. J Natl Cancer Inst 83:288-291, 1991
5. Cortes JE, Pazdur R: Docetaxel. J Clin Oncol 13:2643-2655, 1995
6. Fossella FV, Lee JS, Murphy WK, et al: Phase II study of docetaxel for recurrent or metastatic non-small-cell lung cancer. J Clin Oncol 12:1238-1244, 1994
7. Fossella FV, Lee JS, Shin DM, et al: Phase II study of docetaxel for advanced or metastatic platinum-refractory non-small-cell lung cancer. J Clin Oncol 13:645-651, 1995
8. Gandara DR, Vokes E, Green M, et al: Activity of docetaxel in platinum-treated non-small-cell lung cancer: Results of a phase II multicenter trial. J Clin Oncol 18:131-135, 2000
9. Kunitoh H, Watanabe K, Onoshi T, et al: Phase II trial of docetaxel in previously untreated advanced non-small-cell lung cancer: A Japanese cooperative study. J Clin Oncol 14:1649-1655, 1996
10. Fossella FV, DeVore R, Kerr RN, et al: Randomized phase III trial of docetaxel versus vinorelbine or ifosfamide in patients with advanced non-small-cell lung cancer previously treated with platinum-containing chemotherapy regimens: The TAX 320 Non-Small Cell Lung Cancer Study Group. J Clin Oncol 18:2354-2362, 2000
11. Shepherd FA, Dancey J, Ramlau R, et al: Prospective randomized trial of docetaxel versus best supportive care in patients with non-small-cell lung cancer previously treated with platinum-based chemotherapy. J Clin Oncol 18:2095-2103, 2000
12. Hudis CA, Seidman AD, Crown JP, et al: Phase II and pharmacologic study of docetaxel as initial chemotherapy for metastatic breast cancer. J Clin Oncol 14:58-65, 1996
13. Trudeau ME, Eisenhauer EA, Higgins BP, et al: Docetaxel in patients with metastatic breast cancer: A phase II study of the National Cancer Institute of Canada-Clinical Trials Group. J Clin Oncol 14:422-428, 1996
14. Chan S, Friedrichs K, Noel D, et al: Prospective randomized trial of docetaxel versus doxorubicin in patients with metastatic breast cancer: The 303 Study Group. J Clin Oncol 17:2341-2354, 1999
15. Marre F, Sanderink GJ, de Sousa G, et al: Hepatic biotransformation of docetaxel (Taxotere) *in vitro*: Involvement of the CYP3A subfamily in humans. Cancer Res 56:1296-1302, 1996
16. Nelson DR, Koymans L, Kamataki T, et al: P450 superfamily: Update on new sequences, gene mapping, accession numbers and nomenclature. Pharmacogenetics 6:1-42, 1996
17. Lin JH, Lu AYH: Inhibition and induction of cytochrome P450 and the clinical implications. Clin Pharmacokinet 35:361-390, 1998
18. Parkinson A: An overview of current cytochrome P450 technology for assessing the safety and efficacy of new materials. Toxicol Pathol 24:45-57, 1996
19. Shimada T, Yamazaki H, Mimura M, et al: Interindividual variations in human liver cytochrome P-450 enzymes involved in the oxidation of drugs, carcinogens and toxic chemicals: Studies with liver microsomes of 30 Japanese and 30 Caucasians. J Pharmacol Exp Ther 270:414-423, 1994
20. Guengerich FP: Characterization of human microsomal cytochrome P450 enzymes. Annu Rev Pharmacol Toxicol 29:241-264, 1989
21. Guengerich FP, Turvy CG: Comparison of levels of human microsomal cytochrome P450 enzymes and epoxide hydrolase in normal and disease status using immunochemical analysis of surgical samples. J Pharmacol Exp Ther 256: 1189-1194, 1991
22. Hunt CM, Westerkam WR, Stave GM: Effects of age and gender on the activity of human hepatic CYP3A. Biochem Pharmacol 44: 275-283, 1992
23. Watkins PB, Turgeon DK, Saenger P, et al: Comparison of urinary 6-beta-cortisol and the erythromycin breath test as measures of hepatic P450IIIA (CYP3A) activity. Clin Pharmacol Ther 52:265-273, 1992
24. Kinirons MT, O'Shea D, Downing TE, et al: Absence of correlations among three putative *in vivo* probes of human cytochrome P4503A activity in young healthy men. Clin Pharmacol Ther 54:621-629, 1993
25. Hunt CM, Watkins PB, Saenger P, et al: Heterogeneity of CYP3A isoforms metabolizing erythromycin and cortisol. Clin Pharmacol Ther 51:18-23, 1992
26. Thummel KE, Shen DD, Podoll TD, et al: Use of midazolam as a human cytochrome P450 3A probe: II. Characterization of inter- and intra-individual hepatic CYP3A variability after liver transplantation. J Pharmacol Exp Ther 271:557-566, 1994
27. Thummel KE, Shen DD, Podoll TD, et al: Use of midazolam as a human cytochrome P450 3A probe: I. In vitro-in vivo correlations in liver transplant patients. J Pharmacol Exp Ther 271: 549-556, 1994
28. Hirth J, Watkins PB, Strawderman M, et al: The effect of an individual's cytochrome CYP3A4 activity on docetaxel clearance. Clin Cancer Res 6:1255-1258, 2000
29. Goh BC, Lee SC, Wang LZ, et al: Explaining interindividual variability of docetaxel pharmacokinetics and pharmacodynamics in Asians through phenotyping and genotyping strategies. J Clin Oncol 20:3683-3690, 2002
30. Yamamoto N, Tamura T, Kamiya Y, et al: Correlation between docetaxel clearance and estimated cytochrome P450 activity by urinary metabolite of exogenous cortisol. J Clin Oncol 18:2301-2308, 2000
31. Yamaoka K, Nakagawa T, Uno T: Application of Akaike's information criterion (AIC) in the evaluation of linear pharmacokinetic equations. J Pharmacokinet Biopharm 6:165-175, 1978
32. Nakamura J, Yakata M: Determination of urinary cortisol and 6 beta-hydroxycortisol by high performance liquid chromatography. Clin Chim Acta 149:215-224, 1985
33. Lykkesfeldt J, Loft S, Poulsen HE: Simultaneous determination of urinary free cortisol and 6 beta-hydroxycortisol by high-performance liquid chromatography to measure human CYP3A activity. J Chromatogr B Biomed Appl 660:23-29, 1994
34. Vergniol JC, Bruno R, Montay G, et al: Determination of Taxotere in human plasma by a semi-automated high-performance liquid chromatographic method. J Chromatogr 582:273-278, 1992
35. Taguchi T, Furue H, Niitani H, et al: Phase I clinical trial of RP 56976 (docetaxel) a new anticancer drug. Gan To Kagaku Ryoho 21:1997-2005, 1994
36. Burris H, Irvin R, Kuhn J, et al: Phase I clinical trial of Taxotere administered as either a 2-hour or 6-hour intravenous infusion. J Clin Oncol 11:950-958, 1993
37. Extra JM, Rousseau F, Bruno R, et al: Phase I and pharmacokinetic study of Taxotere (RP 56976; NSC 628503) given as a short

intravenous infusion. Cancer Res 53:1037-1042, 1993

38. Pazdur R, Newman RA, Newman BM, et al: Phase I trial of Taxotere: Five-day schedule. J Natl Cancer Inst 84:1781-1788, 1992

39. Mathijssen RHJ, Verweij J, de Jonge MJ, et al: Impact of body-size measures on irinotecan clearance: Alternative dosing recommendations. J Clin Oncol 20:81-87, 2002

40. De Jongh FE, Verweij J, Loos WJ, et al: Body-surface area-based dosing does not increase accuracy of predicting cisplatin exposure. J Clin Oncol 19:3733-3739, 2001

41. Gurney HP, Ackland S, Gebski V, et al: Factors affecting epirubicin pharmacokinetics and toxicity: Evidence against using body-surface area for dose calculation. J Clin Oncol 16:2299-2304, 1998

42. Loos WJ, Gelderblom H, Sparreboom A, et al: Inter- and intrapatient variability in oral topotecan pharmacokinetics: Implications for body-surface area dosage regimens. Clin Cancer Res 6:2685-2689, 2000

43. Bruno R, Hille D, Riva A, et al: Population pharmacokinetics/pharmacodynamics of docetaxel in phase II studies in patients with cancer. J Clin Oncol 16:187-196, 1998

[CANCER RESEARCH 64, 9101–9104, December 15, 2004]

Small In-Frame Deletion in the Epidermal Growth Factor Receptor as a Target for ZD6474

Tokuzo Arao,[1] Hisao Fukumoto,[1] Masayuki Takeda,[1] Tomohide Tamura,[2] Nagahiro Saijo,[2] and Kazuto Nishio[1,3]

[1]Shien-Lab, [2]Medical Oncology, National Cancer Center Hospital, Tsukiji, Japan; and [3]Pharmacology Division, National Cancer Center Research Institute, Tokyo, Japan

ABSTRACT

ZD6474 is an inhibitor of vascular endothelial growth factor receptor-2 (VEGFR-2/KDR) tyrosine kinase, with additional activity against epidermal growth factor receptor (EGFR) tyrosine kinase. ZD6474 inhibits angiogenesis and growth of a wide range of tumor models *in vivo*. Gefitinib ("Iressa") is a selective EGFR tyrosine kinase inhibitor that blocks signal transduction pathways implicated in cancer cell proliferation. Here, the ability of gefitinib and ZD6474 to inhibit tumor cell proliferation was examined directly in eight cancer cell lines *in vitro*, and a strong correlation was noted between the IC_{50} values of gefitinib and ZD6474 ($r = 0.79$). No correlation was observed between the sensitivity to ZD6474 and the level of EGFR or VEGFR expression. The NSCLC cell line PC-9 was seen to be hypersensitive to gefitinib and ZD6474, and a small (15-bp) in-frame deletion of an ATP-binding site (exon 19) in the EGFR was detected (delE746-A750–type deletion). To clarify the involvement of the deletional mutation of EGFR in the cellular sensitivity to ZD6474, we examined the effect of this agent on HEK293 stable transfectants expressing deletional EGFR that designed as the same deletion site observed in PC-9 cells (293-pΔ15). These cells exhibited a 60-fold higher sensitivity to ZD6474 compared with transfectants expressing wild-type EGFR. ZD6474 inhibited the phosphorylation of the mutant EGFR by 10-fold compared with cells with wild-type EGFR. In conclusion, the findings suggested that a small in-frame deletion in the EGFR increased the cellular sensitivity to ZD6474.

INTRODUCTION

Gefitinib ("Iressa") is an orally active, selective EGFR-tyrosine kinase inhibitor that blocks the signal transduction pathways implicated in the proliferation and survival of cancer cells and other host-dependent processes promoting cancer cell growth (1–3). Mutation of the EGFR tyrosine kinase in human non–small-cell lung carcinoma (NSCLC) and hyperresponsiveness to gefitinib in patients with NSCLC with this mutation recently were reported (4, 5). The mutations were small, in-frame deletions or substitutions clustered around the ATP-binding site in exons 18, 19, and 21 of the EGFR. The mutant receptors were significantly more sensitive to gefitinib than the wild-type receptor (IC_{50} 0.015 versus 0.1 μmol/L). However, of the 95 other primary tumors and 108 cell lines derived from other tumor types studied, none showed any mutations of this receptor (4). Conversely, Ohm *et al.* (6) reported that all four patients with gefitinib-responsive NSCLC were shown to have mutations of the EGFR near the ATP-binding site compared with none of seven cases showing no response to this drug. These results clearly suggest that the EGFR mutation may be a strong determinant of the tumor response to gefitinib.

Received 7/1/04; revised 9/10/04; accepted 10/14/04.

Grant support: Funds for the 2nd Term Comprehensive 10-Year Strategy for Cancer Control and a Grant-in-Aid for Scientific Research from the Ministry of Education, Culture, Sports, Science and Technology of Japan (12217165). T. Arao is the Recipient of a Research Resident Fellowship from the Foundation of Promotion of Cancer Research in Japan.

The costs of publication of this article were defrayed in part by the payment of page charges. This article must therefore be hereby marked *advertisement* in accordance with 18 U.S.C. Section 1734 solely to indicate this fact.

Requests for reprints: Shien-Lab, Medical Oncology, National Cancer Center Hospital, Tsukiji 5-1-1, Chuo-ku, Tokyo 104-0045, Japan. Phone: 81-3-3542-2511; Fax: 81-3-3547-5185; E-mail: knishio@gan2.res.ncc.go.jp.

ZD6474 is an inhibitor of VEGFR-2 and EGFR signaling that inhibits angiogenesis and tumor growth in a diverse range of tumor models (7). We previously have shown that the NSCLC cell line PC-9 is hypersensitive to gefitinib, with an IC_{50} value of ~0.02 μmol/L (8, 9). It subsequently was established that the PC-9 cells also showed hypersensitivity to ZD6474.

In this report, we discuss the presence of an EGFR deletional mutation and its ability to determine sensitivity to ZD6474.

MATERIALS AND METHODS

Reagents. ZD6474 and gefitinib (Iressa) were provided by AstraZeneca (Cheshire, United Kingdom).

Cell Culture. The human NSCLC cell lines PC-9 and PC-14 were established at the Tokyo Medical University (10, 11). The human epidermal carcinoma cell line A431, breast carcinoma cell line SK-BR-3, ovarian carcinoma cell line SK-OV-3, and colon carcinoma cell lines WiDr and LoVo were obtained from the American Type Culture Collection (Manassas, VA). The SBC-3 cells were supplied by Okayama University School of Medicine. All of the cell lines were maintained in Roswell Park Memorial Institute 1640 medium (Sigma, St. Louis, MO) supplemented with 10% heat-inactivated fetal bovine serum (FBS; Life Technologies, Rockville, MD), except for the LoVo (F12; Nissui Pharmaceutical, Tokyo, Japan), WiDr (modified Eagle's medium; Nissui Pharmaceutical), and A431 cells (Dulbecco's modified Eagle's medium; Nissui Pharmaceutical). The HEK293 cell line was obtained from the American Type Culture Collection and cultured in Dulbecco's modified Eagle's medium supplemented with 10% FBS.

***In vitro* Growth-Inhibition Assay.** The cell growth-inhibitory effect of gefitinib and ZD6474 was determined using the thiazolyl blue tetrazolium bromide (MTT) assay (Sigma). Briefly, 180 μL/well of the cell suspension were seeded onto Sumilon 96-well microculture plates (Sumitomo Bakelite, Akita, Japan) and incubated in 10% FBS-containing medium for 24 hours. The cells were treated with gefitinib or ZD6474 at various concentrations (4 nmol/L to 80 μmol/L) and cultured at 37°C in a humidified atmosphere for 72 hours. After the culture period, 20 μL of MTT reagent were added, and the plates were further incubated for 4 hours. After centrifugation of the plates, the culture medium was discarded, and wells were filled with dimethyl-sulfoxide. The absorbance of the cultures was measured at 562 nm using Delta-soft on a Macintosh computer (Apple, Cupertino, CA) interfaced to a Bio-Tek Microplate Reader EL-340 (BioMetallics, Princeton, NJ). This experiment was conducted in triplicate. The statistical analysis was performed using KaleidaGraph (Synergy Software, Reading, PA).

Plasmid Construction and Transfection. Construction of expression plasmid vector of mock (empty vector), wild-type EGFR, and the 15-bp deletional EGFR (delE746-A750–type deletion; ref. 4) that possess the same deletion site observed in PC-9 cells (Fig. 2*A*) in detail was described in another paper.[4] The plasmids were transfected into the HEK293 cells, and the transfectants were selected by Zeosin (Sigma). The stable transfectants (pooled cultures) of the empty vector, wild-type EGFR, and its deletion mutant were designated as Mock, 293-pEGFR, and 293-pΔ15, respectively.

Immunoblot Analysis. Immunoblot analysis was performed as described previously (3). EGFR antibody was purchased from Santa Cruz Biotechnology (no. 1005; Santa Cruz, CA) and Cell Signaling (Beverly, MA). Phospho-EGFR antibody (specific for Tyr-1068), human epidermal growth factor receptor 2, p44/p42 mitogen-activated protein kinase (MAPK), phospho-p44/p42 MAPK, AKT, phospho-AKT, and antirabbit horseradish peroxidase–conjugated antibody all were purchased from Cell Signaling. The transfected cells cultured in

[4] Unpublished observation.

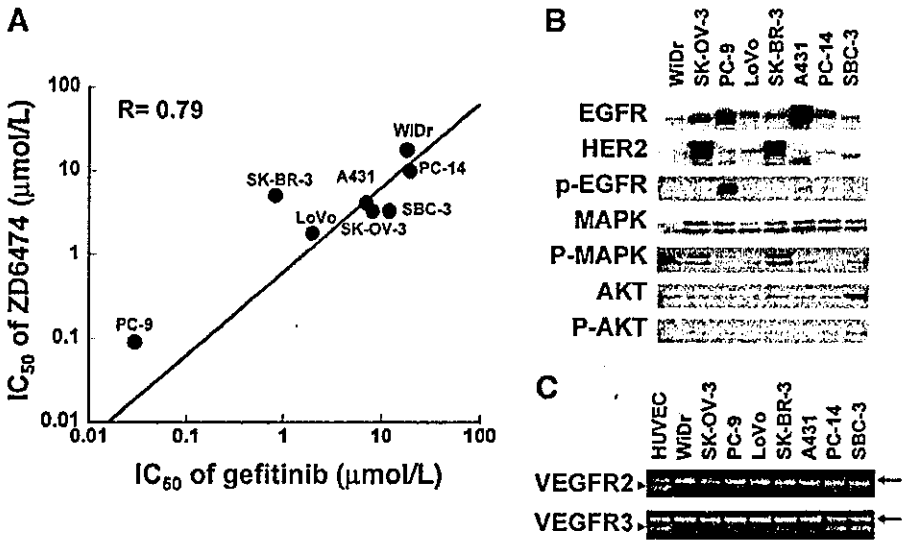

Fig. 1. The cellular characteristics and growth-inhibitory effect of gefitinib and ZD6474. *A*, correlation plot of the IC_{50} values of gefitinib and ZD6474 in human cancer cell lines. The growth-inhibitory effect against PC-9, WiDr, LoVo, PC-14, A431, SK-OV-3, SK-BR-3, and SBC-3 cells was determined by MTT assay (72-hour exposure). The data were obtained from three independent experiments. *B*, expression and phosphorylation status of EGFR and downstream molecules in human cancer cell lines. Data were obtained by immunoblot analysis with anti-EGFR, anti–phospho-EGFR, anti-HER2, anti–phospho-p44/p42 MAPK, anti-p44/p42 MAPK, anti-AKT, anti–phospho-AKT, and anti-AKT. *C*. The mRNA expression level of VEGFR-2 and VEGFR-3 was determined by reverse transcription-PCR. Human umbilical vascular endothelial cell (*HUVEC*) was used as the positive control. Whereas VEGFR-2 expression was not detected in any of the cancer cell lines, VEGFR-3 expression was detected in the PC-14 and SBC-3 cells; *arrows*, β-actin; *arrowheads*, VEGFR-2 or VEGFR-3.

the serum-free medium for 24 hours were stimulated by the addition of EGF (Sigma) at a final concentration of 10 ng/mL. After a 30-minute incubation, the cells were incubated for an additional 3 hours in the presence of ZD6474 and then collected for immunoblot analysis. The subconfluent cancer cell lines were cultured in medium containing 10% FBS and collected for immunoblot analysis.

Reverse-Transcription PCR. Five micrograms of total RNA from each cultured cell line were converted to cDNA using a GeneAmp RNA-PCR kit (Applied Biosystems, Foster City, CA). The primers used for the PCR were as follows: VEGFR-2, 5′-CAGACGGACAGTGGTATGGTTC-3′ (forward) and 5′-ACCTGCTGGTGGAAAGAACAAC-3′ (reverse); and VEGFR-3, 5′-AGCCATTCATCAACAAGCCT-3′ (forward) and 5′-GGCAACAGCTG-GATGTCATA-3′ (reverse). As a control, the following human β-actin primers were used: 5′-GGAAATCGTGCGTGACATT-3′ and 5′-CATCTGCTG-GAAGGTGGACAG-3′. PCR amplification consisted of 35 cycles (95°C for 45 seconds, 62°C for 45 seconds, and 72°C for 60 seconds) followed by incubation at 72°C for 7 minutes. The bands were visualized by ethidium bromide staining.

Sequencing. Sequencing of exons 18 through 21 of EGFR cDNA in the tumor cell lines was performed. The cDNAs were amplified using the following primers: 5′-TCCAAACTGCACCTACGGATGC-3′ (forward) and 5′-CATCAACTCCCAAACGGTCACC-3′ (reverse). PCR amplification consisted of 25 cycles (95°C for 45 seconds, 55°C for 30 seconds, and 72°C for 60 seconds). The sequences of the PCR products were determined using ABI prism 310 (Applied Biosystems). Amplification and sequencing were performed in duplicate for each tumor cell line. The sequences were compared with the GenBank-archived human sequence of EGFR (accession no. NM 005228.3).

RESULTS

Growth-Inhibitory Activity of Gefitinib and ZD6474. We examined the *in vitro* growth-inhibitory activities of gefitinib and ZD6474 on eight cancer cell lines by MTT assay. The IC_{50} values of gefitinib and ZD6474 for each cell line were compared and plotted as shown in Fig. 1A. Good correlation ($r = 0.79$) was observed between the IC_{50} values of gefitinib and ZD6474, suggesting that the mechanisms underlying the growth-inhibitory activities of the two drugs *in vitro* might be similar. To clarify the correlation between the cellular sensitivity for gefitinib and ZD6474 and the EGFR status, we examined the expression and phosphorylation levels of EGFR in the cell lines by immunoblot analysis (Fig. 1*B*). No correlation was found between the expression status or the phosphorylation level of EGFR and the IC_{50} value of either drug. There also was no correlation between the cellular sensitivity and the phosphorylation status of any downstream molecules, such as phosphorylated MAPK and phospho-AKT (Fig. 1*B*). To determine the correlation between the VEGFR expression levels and cellular sensitivity, we examined the mRNA levels of the VEGFR-2 and VEGFR-3 in the cell lines by reverse transcription-PCR and detected VEGFR-3 transcripts in PC-14 and SBC-3 cells (Fig. 1*C*). VEGFR-2 was not detectable in all of the cancer cell lines. The results suggested that there was no correlation between the cellular sensitivity to ZD6474 and the VEGFR-2 and VEGFR-3 expression level. Among all of the cell lines examined, the PC-9 cell line was found to be hypersensitive to gefitinib (IC_{50} = 0.03 ± 0.002 μmol/L) and ZD6474 (IC_{50} values = 0.09 ± 0.01 μmol/L). The respective IC_{50} values of gefitinib and ZD6474 for the other cell lines were as follows: WiDr, 18.7 ± 2.5 μmol/L and 17.7 ± 2.3 μmol/L; SK-OV-3, 8.3 ± 1.5 μmol/L and 3.3 ± 0.2 μmol/L; LoVo, 2.0 ± 0.3 μmol/L and 1.8 ± 0.2 μmol/L; A431, 7.1 ± 0.9 μmol/L and 4.1 ± 0.2 μmol/L; PC-14, 20 ± 2.1 μmol/L and 10 ± 1.2 μmol/L; SK-BR-3, 0.8 ± 0.15 μmol/L and 5.2 ± 0.1 μmol/L; and SBC-3, 12.3 ± 2.1 μmol/L and 3.3 ± 0.3 μmol/L.

Fifteen-Base Pair In-Frame Deletion of EGFR in PC-9 Cells. To determine the cellular determinants of the hypersensitivity of the PC-9 cells to gefitinib, we determined the sequence of the EGFR mRNA in the PC-9 cells. The analysis revealed a 15-bp in-frame deletion around the ATP-binding site in exon 19 (Fig. 2*A*). No deletion or mutation was found in the other cell lines. The 15-bp in-frame deletion in the EGFR was consistent with the observations of Ohm *et al.* (6) in four patients with lung cancer.

Deletional Mutation of EGFR Increases the Cellular Sensitivity to ZD6474. We hypothesized that the cellular hypersensitivity of the PC-9 cells to ZD6474 was attributable to the deletional mutation of EGFR in these cells. To confirm the validity of this hypothesis, we examined ZD6474 sensitivity to HEK293 transfectant expressing the 15-bp deletion mutant EGFR or wild-type EGFR. The sequencing of EGFR cDNA obtained from 293-pEGFR and 293-pΔ15 cells was shown (Fig. 2*B*). The sensitivity of the transfectants was examined by 72-hour exposure of ZD6474 using MTT assay. The 293-pΔ15 cells were found to be 60-fold more sensitive to ZD6474 than the mock and wild-type EGFR transfectants (Fig. 3*A*). The IC_{50} of ZD6474 for the 293-pΔ15 cells, 293-pEGFR cells, and the mock transfectants were 0.08, 5.2, and 6.3 μmol/L, respectively.

The EGFR expression levels in the transfectants were quantified by immunoblot analysis using anti-EGFR antibody recognizing the

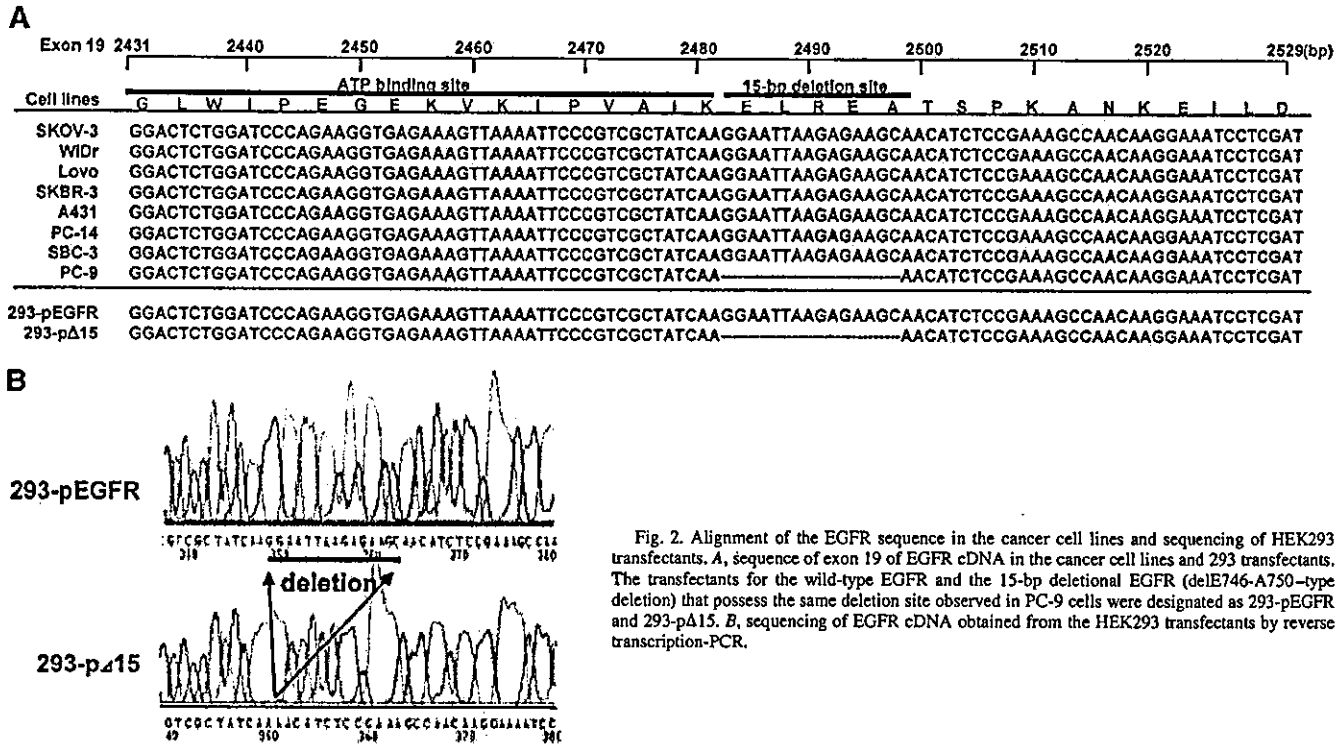

Fig. 2. Alignment of the EGFR sequence in the cancer cell lines and sequencing of HEK293 transfectants. *A*, sequence of exon 19 of EGFR cDNA in the cancer cell lines and 293 transfectants. The transfectants for the wild-type EGFR and the 15-bp deletional EGFR (delE746-A750–type deletion) that possess the same deletion site observed in PC-9 cells were designated as 293-pEGFR and 293-pΔ15. *B*, sequencing of EGFR cDNA obtained from the HEK293 transfectants by reverse transcription-PCR.

COOH-terminus of EGFR. High expression of EGFR proteins was detected in the 293-pΔ15 cells and 293-pEGFR cells but not in the mock cells (Fig. 3*B*). Exposure to ZD6474 did not affect the expression of levels of either the wild-type or the mutant EGFR. EGFR status was quantified by measuring the phosphorylation level of the Tyr-1068 residue, commonly used as a marker of the autophosphorylation of EGFR (12).

Under the condition of serum starvation, wild-type EGFR did not show any autophosphorylation, whereas the addition of EGF activated the receptor. However, marked autophosphorylation of the mutant EGFR was observed, even without the addition of EGF (Fig. 3*B*). ZD6474 exposure inhibited the phosphorylation of wild-type EGFR and mutant EGFR in a dose-dependent manner, with 2 μmol/L and 0.2 μmol/L of ZD6474 completely inhibiting phosphorylation of the wild-type EGFR and mutant EGFR, respectively. These results suggest that cells expressing the deletion mutant of EGFR are markedly more sensitive to the inhibitory effect of ZD6474 than those expressing wild-type EGFR.

DISCUSSION

Recent reports by Paez and Lynch have indicated that deletional mutations of EGFR impact on the therapeutic effects of the molecular-

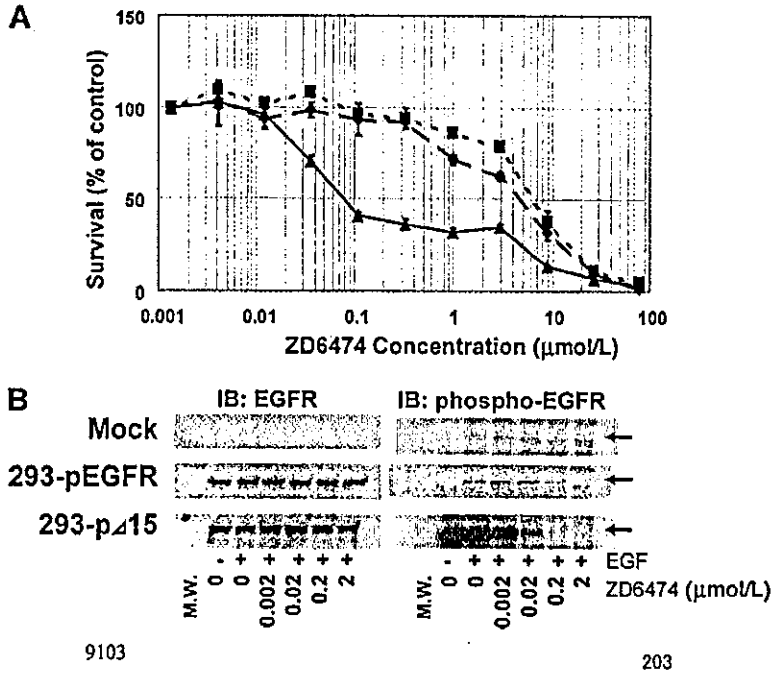

Fig. 3. Effect of ZD6474 on cellular growth inhibition and phosphorylated status of EGFR in the HEK293 transfectants. *A*. The cellular sensitivity of the transfectants against ZD6474 was determined by MTT assay (72-hour exposure). The mean values and SD represent the values obtained from the growth-inhibition curves in three independent experiments; ♦, mock (empty vector); ■, 293-pEGFR (wild-type EGFR); ▲, 293-pΔ15 (deletional-mutant EGFR). *B*, effect of EGF stimulation and ZD6474 exposure on mock, wild-type EGFR, and deletional mutant EGFR-transfected HEK293 cells determined by immunoblot analysis. Cells cultured under serum starvation for 24 hours were exposed to 10 ng/mL EGF for 30 minutes and then treated with 0.002 to 2 μmol/L ZD6474 for 3 hours in the presence or absence of EGF. *Left*, EGFR expression levels; *right*, EGFR phosphorylation levels.

targeted EGFR inhibitor gefitinib (4, 5). Here, we show that a 15-bp deletional mutation residing near the ATP binding site of EGFR in cancer cells also increases the sensitivity of the cells to ZD6474.

ZD6474 is a small molecule inhibitor of VEGFR-2 tyrosine kinase that is in Phase II clinical evaluation. *In vivo*, this compound inhibits VEGF signaling, tumor-induced angiogenesis, and the growth of a histologically diverse panel of tumor xenografts. This includes highly significant activity against tumor xenografts with intrinsic or acquired resistance to EGFR inhibitors (13). However, ZD6474 also has activity against EGFR tyrosine kinase that may give additional therapeutic benefit when tumors have a high dependency on EGFR signaling for growth and/or survival. This has been shown in PC-9 cells that are hypersensitive to treatment with gefitinib (9). PC-9 tumor cells also are hypersensitive to ZD6474 *in vitro* and regress in response to ZD6474 treatment when grown as tumor xenografts *in vivo* (14).

We have shown that PC-9 cells contain a 15-bp in-frame deletional mutation in EGFR, and this mutation may confer increased sensitivity to ZD6474 and gefitinib. The difference in ZD6474 concentration required for complete inhibition of wild-type and mutant EGFR phosphorylation was relatively small (2 versus 0.2 μmol/L), whereas difference in sensitivity to ZD6474 was large (60-fold).

The deletional EGFR was constitutively phosphorylated, and the addition of EGF to the cultures did not result in any additional increase in phosphorylation (Fig. 3*B*). These observations contradict data reported by Lynch *et al.* (4), who showed that a receptor with a similar deletion was still regulated by EGF.

The most possible explanation for this contradiction is that the expression level of deletional EGFR in the 293-pΔ15 cells is much higher than that of the transient transfectant of Del L747-P753insS reported by Lynch *et al.* Ligand-independent oligomerization of the receptor and phosphorylation may have occurred in the 293-pΔ15 cells as a result. This hypothesis is consistent with the result that PC-9 cells harboring the same 15-bp deletion showed a stronger phosphorylation of the EGFR in a 10% FBS medium than other nonhypersensitive cell lines (Fig. 1*B*).

The other possible explanation is that apparent distinct amino acid sequences of EGFR exist between our mutant and that of Lynch *et al.* (293-pΔ15, VAIKELREATSPK>VAIKTSPK; delL747-P753insS, VAIKELREATSPK>VAIKESK). Five amino acids are simply deleted in the 293-pΔ15 cells, whereas six amino acids are deleted and serine is inserted in the delL747-P753insS cells. This small difference may be critical to the ATP-binding properties of 293-pΔ15 and delL747-P753insS, determining whether EGFR is constitutively active. Therefore, it is not surprising that our constitutive active form of EGFR is out of ligand regulation.

The mock-transfected 293 cells and 293-pEGFR cells were not sensitive to the growth-inhibitory effect of ZD6474 (Fig. 3*A*), indicating that these cells were independent of EGFR signaling. The 293 cells are oncogenic transformant. Therefore, the 293 cells were considered to have acquired the dependency on the oncogenic signal. Conversely, the overexpression of the deletional EGFR transduces the excess signal to downstream of EGFR in the 293-pΔ15 cells. If the downstream mutant EGFR signaling pathway were shared with that of the oncogenic signaling pathway in the cells, the excess and constitutive signal from the mutant EGFR would dominate the downstream pathway, possibly influencing the dependency of the cells on the EGFR signal.

A recent report by Sordella *et al.* (15) showed the mutant EGFRs (delL747-P753insS and L858R) expressing a stable transfectant selectively activate AKT and STAT signaling pathways. They also showed that NSCLC cell lines that harboring mutant EGFR transduce survival signals and depend on the acquisition of these signals. Their evidence is consistent with our present speculations. We now are investigating the downstream pathways of the mutant EGFR signaling in the 293-pΔ15 cells.

In summary, inhibition of VEGFR-2 tyrosine kinase by ZD6474 may potentially confer activity against tumors that are not dependent on EGFR signaling. Nevertheless, the additional activity of ZD6474 against EGFR tyrosine kinase could provide further benefit, particularly when EGFR is mutated. Patients with lung adenocarcinoma showing EGFR mutations are likely to be highly sensitive to gefitinib and ZD6474 treatment.

REFERENCES

1. Ciardiello F, Caputo R, Tortora G, et al. Antitumor effect and potentiation of cytotoxic drugs activity in human cancer cells by ZD-1839 (Iressa), an epidermal growth factor receptor-selective tyrosine kinase inhibitor. Clin Cancer Res 2000;6: 2053–63.
2. Moasser MM, Basso A, Averbuch SD, Rosen N. The tyrosine kinase inhibitor ZD1839 ("Iressa") inhibits HER2-driven signaling and suppresses the growth of HER2-overexpressing tumor cells. Cancer Res 2001;61:7184–8.
3. Koizumi F, Kanzawa F, Nishio K, et al. Synergistic interaction between the EGFR tyrosine kinase inhibitor gefitinib ("Iressa") and the DNA topoisomerase I inhibitor CPT-11 (irinotecan) in human colorectal cancer cells. Int J Cancer 2004;108:464–72.
4. Lynch TJ, Bell DW, Haber DA, et al. Activating mutations in the epidermal growth factor receptor underlying responsiveness of non-small-cell lung cancer to gefitinib. N Engl J Med 2004;350:2129–39.
5. Paez JG, Janne PA, Meyerson M, et al. EGFR mutations in lung cancer: correlation with clinical response to gefitinib therapy. Science 2004;304:1497–500.
6. Ohm JE, Amann JM, Carbone DP. Acquired EGFr TKI resistance associated with mutation of the EGFr. Presented at the 95th Annual Meeting of the American Association of Cancer Research, November 17–21, 2004, Bonita Springs, FL.
7. Ciardiello F, Caputo R, Tortora G, et al. Antitumor effects of ZD6474, a small molecule vascular endothelial growth factor receptor tyrosine kinase inhibitor, with additional activity against epidermal growth factor receptor tyrosine kinase. Clin Cancer Res 2003;9:1546–56.
8. Naruse I, Ohmori T, Nishio K, et al. Antitumor activity of the selective epidermal growth factor receptor-tyrosine kinase inhibitor (EGFR-TKI) Iressa (ZD1839) in an EGFR-expressing multidrug-resistant cell line in vitro and in vivo. Int J Cancer 2002;98:310–5.
9. Koizumi F, Taguchi F, Shimoyama T, Saijo N, Nishio K. Mechanism of resistance to epidermal growth factor receptor inhibitor ZD1839: a role for inhibiting phosphorylation of EGFR at Tyr1068. Presented at the 94th Annual Meeting of the American Association of Cancer Research, July 11–14, 2003, Washington, DC.
10. Kawamura-Akiyama Y, Kusaba H, Nishio K, et al. Non-cross resistance of ZD0473 in acquired cisplatin-resistant lung cancer cell lines. Lung Cancer 2002;38:43–50.
11. Nishio K, Arioka H, Saijo N, et al. Enhanced interaction between tubulin and microtubule-associated protein 2 via inhibition of MAP kinase and CDC2 kinase by paclitaxel. Int J Cancer 1995;63:688–93.
12. Nielsen UB, Cardone MH, Sinskey AJ, MacBeath G, Sorger PK. Profiling receptor tyrosine kinase activation by using Ab microarrays. Proc Natl Acad Sci USA 2003;100:9330–5.
13. Ciardiello F, Bianco R, Tortora G, et al. Antitumor activity of ZD6474, a vascular endothelial growth factor receptor tyrosine kinase inhibitor, in human cancer cells with acquired resistance to antiepidermal growth factor receptor therapy. Clin Cancer Res 2004;10:784–93.
14. Taguchi F, Koh Y, Nishio K, et al. Anticancer effects of ZD6474, a VEGF receptor tyrosine kinase inhibitor, in gefitinib (Iressa) sensitive and resistant xenograft models. Cancer Sci 2004;in press.
15. Sordella R, Bell DW, Haber DA, Settleman J. Gefitinib-sensitizing EGFR mutations in lung cancer activate anti-apoptotic pathways. Science 2004;305:1163–7.

Anticancer effects of ZD6474, a VEGF receptor tyrosine kinase inhibitor, in gefitinib ("Iressa")-sensitive and resistant xenograft models

Fumiko Taguchi,[1] Yasuhiro Koh,[1] Fumiaki Koizumi,[1,2] Tomohide Tamura,[3] Nagahiro Saijo[3] and Kazuto Nishio[1,2,4]

[1]Pharmacology Division, National Cancer Center Research Institute; and [2]Shien-Lab and [3]Medical Oncology, National Cancer Center Hospital, 5-1-1 Tsukiji, Chuo-ku, Tokyo 104-0045

(Received August 6, 2004/Revised September 27, 2004/Accepted October 8, 2004)

ZD6474 is a novel, orally available inhibitor of vascular endothelial growth factor (VEGF) receptor-2 (KDR) tyrosine kinase, with additional activity against epidermal growth factor receptor (EGFR) tyrosine kinase. ZD6474 has been shown to inhibit angiogenesis and tumor growth in a range of tumor models. Gefitinib ("Iressa") is an selective EGFR tyrosine kinase inhibitor (TKI) that blocks signal transduction pathways. We examined the antitumor activity of ZD6474 in the gefitinib-sensitive lung adenocarcinoma cell line, PC-9, and a gefitinib-resistant variant (PC-9/ZD). PC-9/ZD cells showed cross-resistance to ZD6474 in an *in vitro* dye formation assay. In addition, ZD6474 showed dose-dependent inhibition of EGFR phosphorylation in PC-9 cells, but inhibition was only partial in PC-9/ZD cells. ZD6474-mediated inhibition of tyrosine residue phosphorylation (Tyr992 and Tyr1045) on EGFR was greater in PC-9 cells than in PC-9/ZD cells. These findings suggest that the inhibition of EGFR phosphorylation by ZD6474 can contribute a significant, direct growth-inhibitory effect in tumor cell lines dependent on EGFR signaling for growth and/or survival. The effect of ZD6474 (12.5–50 mg/kg/day p.o. for 21 days) on the growth of PC-9 and PC-9/ZD tumor xenografts in athymic mice was also investigated. The greatest effect was seen in gefitinib-sensitive PC-9 tumors, where ZD6474 treatment (>12.5 mg/kg/day) resulted in tumor regression. Dose-dependent growth inhibition, but not tumor regression, was seen in ZD6474-treated PC-9/ZD tumors. These studies demonstrate that the additional EGFR TKI activity may contribute significantly to the antitumor efficacy of ZD6474, in particular in those tumors that are dependent on continued EGFR-signaling for proliferation or survival. In addition, these results provide a preclinical rationale for further investigation of ZD6474 as a potential treatment option for both EGFR-TKI-sensitive and EGFR-TKI-resistant tumors. (Cancer Sci 2004; 95: 984–989)

ZD6474 is a novel, orally available inhibitor of VEGF receptor-2 (KDR) tyrosine kinase, with additional activity against EGFR tyrosine kinase, and it inhibits angiogenesis and tumor growth in a diverse range of tumor models.[1,2] Phase I clinical evaluation has shown ZD6474 to be generally well tolerated, and tumor responses in patients with non-small cell lung cancer (NSCLC) have been documented.[3,4] Thus, ZD6474 is considered to be a multi-target tyrosine kinase inhibitor active against solid tumors. The purpose of this study is to clarify the mode of antitumor action of ZD6474 as compared with that of gefitinib ("Iressa," ZD1839). Gefitinib is an orally active, selective EGFR tyrosine kinase inhibitor (EGFR-TKI) that blocks signal transduction pathways implicated in the proliferation and survival of cancer cells and other host-dependent processes promoting tumor growth.[5–7] Gefitinib is now available clinically for non-small cell lung cancer patients. In order to elucidate the mode of action of ZD6474, the antitumor activity and pharmacodynamics were investigated in an established human lung cancer cell line resistant to gefitinib (PC-9/ZD cells).[8] This approach allowed us to clarify the common and differential modes of actions of gefitinib and ZD6474 in lung cancer, and this will be important for deciding how to use ZD6474 in non-small cell lung cancer patients in combination with gefitinib.

Materials and Methods

Reagents and cell culture. ZD6474 and gefitinib ("Iressa," ZD1839) were provided by AstraZeneca (Macclesfield, UK). Human NSCLC cell lines PC-9 and PC-14 were used.[9,10] In addition, a gefitinib-resistant subline, PC-9/ZD, was derived from PC-9 cells by short-term exposure to the mutagen *N*-methyl-*N'*-nitro-*N*-nitrosoguanidine, continuous exposure to 0.2–0.5 μ*M* gefitinib for 28 days, and subcloning. The resistant phenotype has been stable for at least 6 months under drug-free conditions.[8] The PC-9/ZD cell line shows no cross-resistance to conventional anticancer drugs.[8] Cells were maintained in RPMI-1640 (Sigma Chemical Co., St. Louis, MO) supplemented with 10% heat-inactivated fetal bovine serum (Gibco BRL, Grand Island, NY).

Antibodies. Anti-vonWillebrand Factor (vWF) antibody was purchased from Chemicon, Temecula, CA. Affinity-purified antibody to EGFR was purchased from Santa Cruz, CA and affinity-purified antibodies to phospho-EGFR specific for Tyr845, Tyr992, Tyr1045, and Tyr1068 were purchased from Cell Signaling Technology, Beverly, MA.

Growth inhibition assay. Cell sensitivity to ZD6474 and gefitinib was estimated by means of the 3-(4,5-dimethylthiazol-2-yl)-2,5-diphenyltetrazolium bromide (MTT) assay as described previously.[11] Briefly, PC-9, PC-9/ZD, or PC-14 cells were exposed to 0–10 μ*M* ZD6474 or gefitinib for 72 h before measuring absorbance. Optical density was assessed at 562–630 nm using an EL340 96-well microtiter plate reader (Bio-Tek, Winooski, VT).

Xenograft studies in athymic mice. Suspensions of PC-9 cells (5×10^6) or PC-9/ZD cells (3×10^6) were injected subcutaneously into the backs of 5-week-old female athymic mice (Japan Charles River Co., Atsugi, Japan). After 1 week (tumors >95 mm^3), mice were randomly allocated into groups of six animals to receive ZD6474 (12.5, 25, or 50 mg/kg/day), gefitinib (12.5, 25, or 50 mg/kg/day) or vehicle only by oral gavage. Tumor diameter and body weight were measured twice weekly. The tumor volume was calculated (width^2×length/2) and is presented as a percentage of the pretreatment value. A tumor volume below 100% of the pretreatment volume was defined as "tumor reduction." Experiments were performed in accordance with the UK Coordinating Committee on Cancer Research Guidelines for the welfare of animals in experimental neoplasia (second edition). After 3 weeks of treatment, tumors were removed.

[4]To whom correspondence should be addressed.
E-mail: knishio@gan2.res.ncc.go.jp

Abbreviations: VEGF, vascular endothelial growth factor; EGFR, epidermal growth factor receptor; TKI, tyrosine kinase inhibitor; NSCLC, non-small cell lung cancer; MTT, 3-(4,5-dimethylthiazol-2-yl)-2,5-diphenyltetrazolium bromide.

Two tumor specimens per group were processed for immunohistochemical analysis.

Immunohistochemical analysis. Immunohistochemistry was performed on formalin-fixed, paraffin-embedded tissue sections as reported previously.[1,5] An anti-Ki67 monoclonal antibody (clone MIB1; DBA, Milan, Italy) was used and the proportion of positive (proliferating) cells was assessed. At least 1000 cancer cells were counted and scored per slide. Both the percentage of specifically stained cells and the intensity of immunostaining were recorded. Blood vessels were detected with an anti-von Willebrand Factor (vWF) antibody (Chemicon). Microvessel density was determined by calculating the proportion of vWF-positive cells.

Evaluation of apoptosis (TUNEL). Sections were stained with an *in situ* Death Detection POD Kit (Roche Diagnostic GmbH, Mannheim, Germany) according to the manufacturer's instructions. At least 1000 tumor cell nuclei from the most evenly and distinctly labeled areas were examined. The TUNEL-positive tumor cell nuclei were counted, and the apoptotic index was calculated as the proportion of cells with apoptotic nuclei.

Immunoprecipitation and immunoblotting. Cells were maintained in medium without serum for 12 h. Then serum-starved cells were exposed to ZD6474 or gefitinib, incubated for 1 h and stimulated in medium including 10% fetal bovine serum for 30 min. The cells were subsequently washed twice with ice-cold PBS, scraped in lysis buffer (50 m*M* Tris-HCl [pH 8.0], 120 m*M* NaCl, 0.5% Nonidet P-40, 100 m*M* NaF, 200 μ*M* Na_3VO_4, and 10 μg/ml each of aprotinin, leupeptin, and PMSF), and incubated on ice for 60 min. The lysates were centrifuged at 8000*g* for 20 min, and total protein was obtained from the supernatants. Protein concentration was measured with the bicinchoninic acid protein assay (Pierce, Rockford, IL). Cell lysates for immunoprecipitates contained 2 mg of total protein. Anti-EGFR antibody (3 μg) was incubated overnight with the lysates at 4°C, and the precipitates were collected with 40 μliters of Protein G Sepharose beads over a 1 h period. Antibody-complexed proteins were washed with lysis buffer, analyzed by SDS-PAGE and visualized using an enhanced chemiluminescence solution (ECL; Amersham Pharmacia Biotech UK, Buckinghamshire, UK). Quantative analysis was performed using Kodak software. Quantified values of phospho-EGFR bands were standardized according to those of EGFR bands.

Results

***In vitro* evaluation of ZD6474 and gefitinib inhibition of tumor cell growth.** The IC_{50} values of gefitinib for growth inhibition of PC-9 and PC-9/ZD cells were 0.038 μ*M* and 6.8 μ*M*, respectively. The IC_{50} values of ZD6474 were 0.14 μ*M* and 5.92 μ*M*, respectively (Fig. 1A). PC-9 cells were 180-fold more sensitive to gefitinib than PC-9/ZD cells, and PC-9/ZD cells were cross-resistant to ZD6474. Experiments with another VEGFR-TKI, SU5416, and PDGFR-TKI, Tyrphostin 9, revealed no cross-resistance (data not shown).

In a separate experiment, the IC_{50} values of gefitinib were 0.006 μ*M* and 20.5 μ*M*, in PC-9 and PC-14 (another human NSCLC cell line), respectively (Fig. 1B). PC-9 cells were therefore approximately 3400-fold more sensitive to gefitinib than PC-14 cells. Corresponding IC_{50} values for ZD6474 were 0.11 μ*M* and 9.81 μ*M*, demonstrating cross-resistance to ZD6474.

Other workers have examined the ability of gefitinib or ZD6474 to inhibit serum-dependent tumor cell growth *in vitro*, and have demonstrated IC_{50} values of gefitinib[12] and ZD6474[13] of >1 μ*M* for tumor cell lines. Therefore, PC-9 is particularly sensitive to *in vitro* growth inhibition by both gefitinib and ZD6474, whereas the sensitivities of both gefitinib-resistant PC-9/ZD and PC-14 fall within the normal range reported for other tumor cell lines.

***In vivo* antitumor effects.** ZD6474 treatment (12.5–50 mg/kg/day) resulted in inhibition of PC-9 tumor growth, with robust tumor regression seen even at the lowest dose tested. ZD6474 treatment also resulted in dose-dependent inhibition of PC-9/ZD tumor xenograft growth, although in this case, regression was not seen (Fig. 2, A and B). This antitumor effect of ZD6474 was very similarly to that of gefitinib we previously reported (Fig. 2, C and D).[8]

Effect of treatment on cell proliferation, apoptosis, and vascularization. ZD6474 treatment resulted in a dose-dependent decrease in the proportion of proliferating cells in the PC-9 tumors, but not in PC-9/ZD xenografts (Fig. 3). No significant

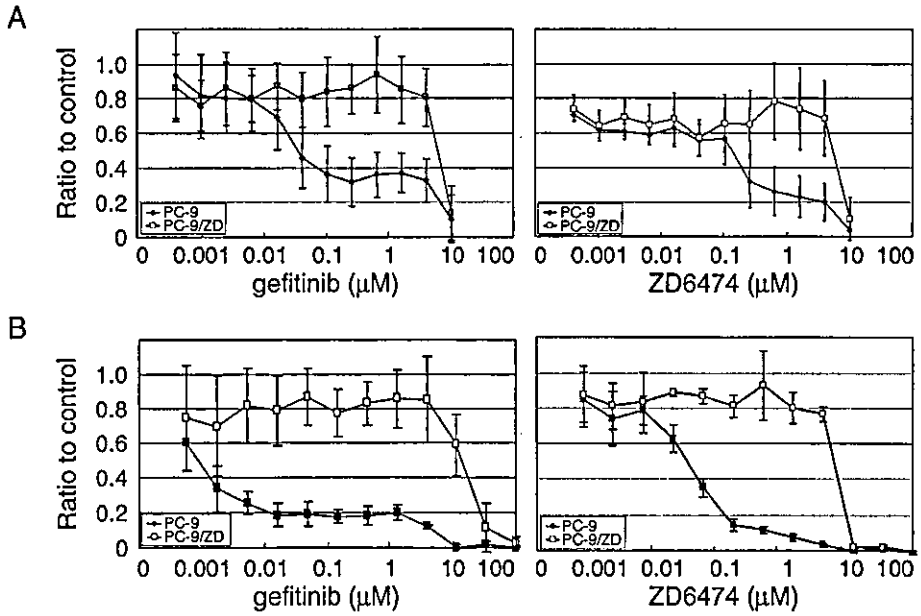

Fig. 1. Growth inhibitory effect of gefitinib (ZD1839) and ZD6474. A: PC-9 and PC-9/ZD, B: PC-9 and PC-14 cells. Data shown are mean values from three experiments (±SD).

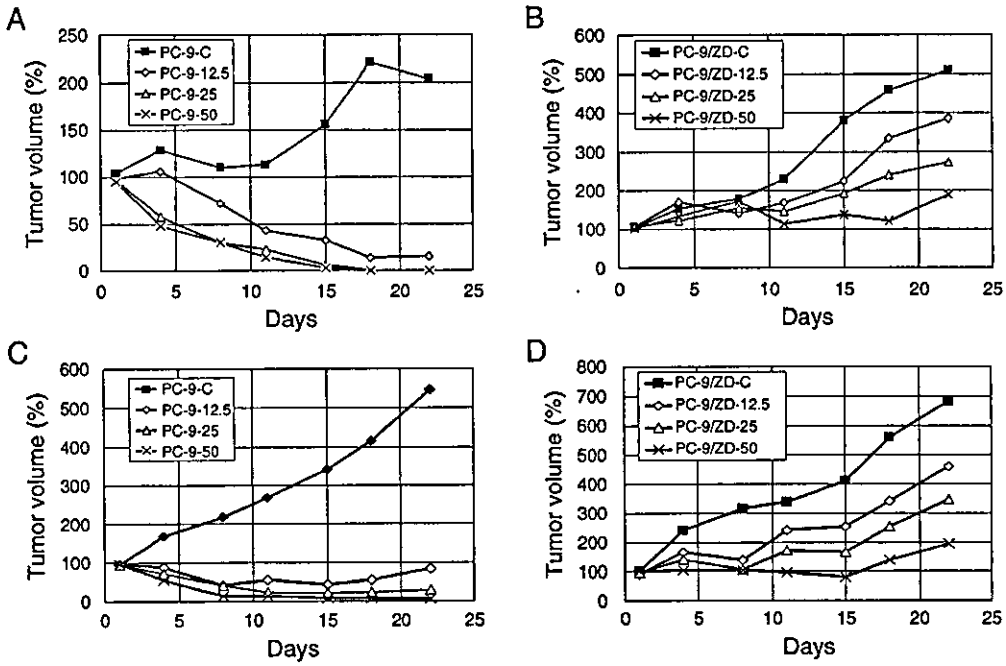

Fig. 2. Antitumor activity of ZD6474 (A, B) and gefitinib (C, D) on established PC-9 (A, C) and PC-9/ZD (B, D) human lung cancer xenografts.

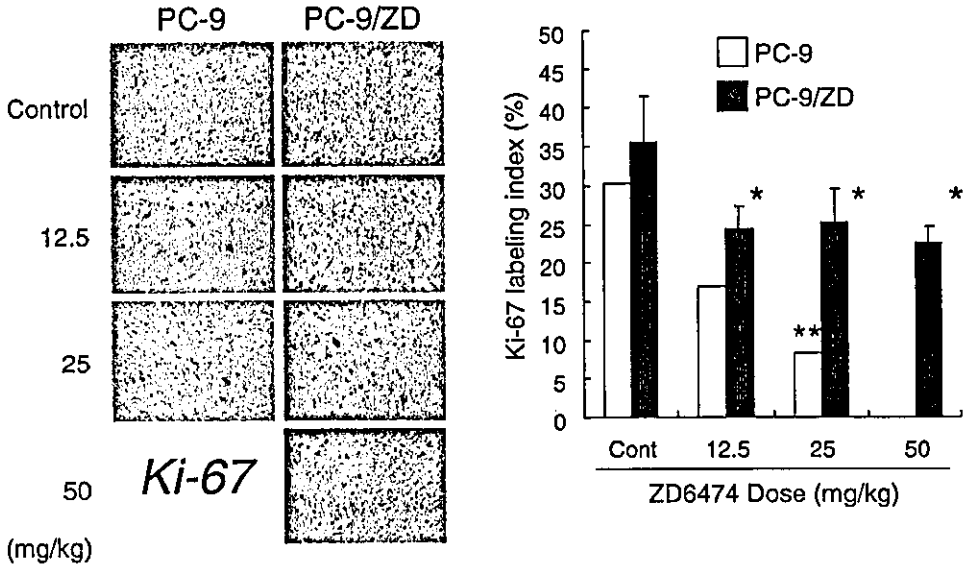

Fig. 3. Effect of ZD6474 on the Ki67 labeling index of PC-9 and PC-9/ZD tumors *in vivo*. Data represent mean values (±SD). Significant difference from control shown by the Dunnett test (* $P<0.05$, ** $P<0.01$).

increase in apoptosis was observed in either tumor type (Fig. 4).

Assessment of tumor vascularization showed a significant reduction in vascular density following ZD6474 treatment of PC-9 tumor xenografts, although no effect was seen in PC-9/ZD tumors (Fig. 5). Differences in the action of ZD6474 on PC-9 and PC-9/ZD tumors are summarized in Table 1.

Inhibition of EGFR activity. It is possible that the antitumor activity of ZD6474 is partly attributable to EGFR inhibition based on the evidence of cross-resistance to gefitinib (Figs. 1–3). Therefore, site-specific anti-phosphorylated-EGFR antibodies were used to investigate inhibition of EGFR phosphorylation by ZD6474 in PC-9 and PC-9/ZD cells at four different tyrosine phosphorylation sites (Tyr845, Tyr992, Tyr1045, and Tyr1068; Fig. 6). ZD6474 dose-dependently inhibited phosphorylation of the four EGFR tyrosine residues in PC-9 cells (Fig. 6). In PC-9/ZD cells, drug-related inhibition of phosphorylation at the Tyr992 site was highly resistant to ZD6474 treatment (Fig. 6), and the Tyr845 and Tyr1045 sites were moderately resistant, while the effect of phosphorylation at the Tyr1068 site did not differ significantly between the sensitive and resistant cell lines (Table 1). The spectrum of activity of ZD6474 on the

four EGFR tyrosine residues examined in PC-9/ZD cells differed from that of gefitinib. ZD6474 displayed a variety of actions on each tyrosine residue, which may be responsible for the wide range of biological activities.

Discussion

In the NSCLC xenograft model reported here, ZD6474 treatment significantly inhibited PC-9 tumor growth, inducing tumor regression. In addition, ZD6474 caused dose-dependent PC-9/ZD tumor growth inhibition. These data indicate that ZD6474 exerts potent antitumor activity against gefitinib-sensitive and resistant lung cancers *in vivo*. Although PC-9/ZD cells are less sensitive to gefitinib than PC-9 cells, the *in vitro* sensitivity of these cells falls within the normal range for other tumor cell lines. Accordingly, gefitinib has significant *in vivo* activity against PC-9/ZD, producing a dose-dependent inhibition of xenograft growth, rather than the tumor regression seen with PC-9 xenografts. Therefore, the antitumor activity of ZD6474 appeared to parallel that of gefitinib in PC-9 and PC-9/ZD tumor cells, both *in vitro* and *in vivo*. Since gefitinib is a TKI with a high degree of selectivity for EGFR,[1,2,4] inhibition of EGFR autophosphorylation is likely to contribute to the antitumor activity of ZD6474, particularly in tumor cells which are dependent on EGFR signaling for continued growth and survival. This was shown *in vitro*, as ZD6474 inhibited EGFR

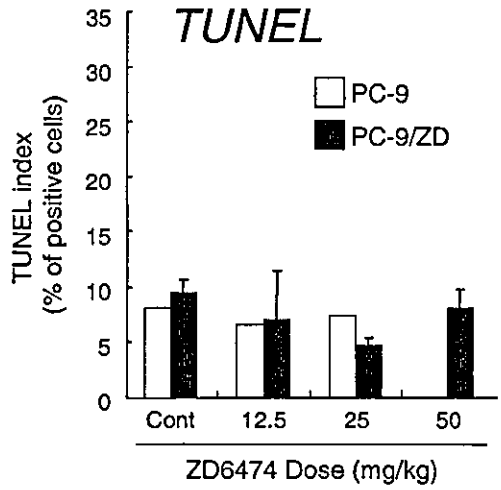

Fig. 4. Effect of ZD6474 on the TUNEL index of PC-9 or PC-9/ZD tumors *in vivo*. Data represent mean values (±SD).

Table 1. Site-specific effect of ZD6474 on EGFR tyrosine residues in PC-9 and PC-9/ZD cells

Tyr residue of EGFR	Inhibition of phosphorylation			
	ZD6474		Gefitinib	
	PC-9	PC-9/ZD	PC-9	PC-9/ZD
845	++	+	++	+
992	++	–	++	++
1045	++	+	–	–
1068	++	++	++	+

++ strong; + moderate; – not significant.

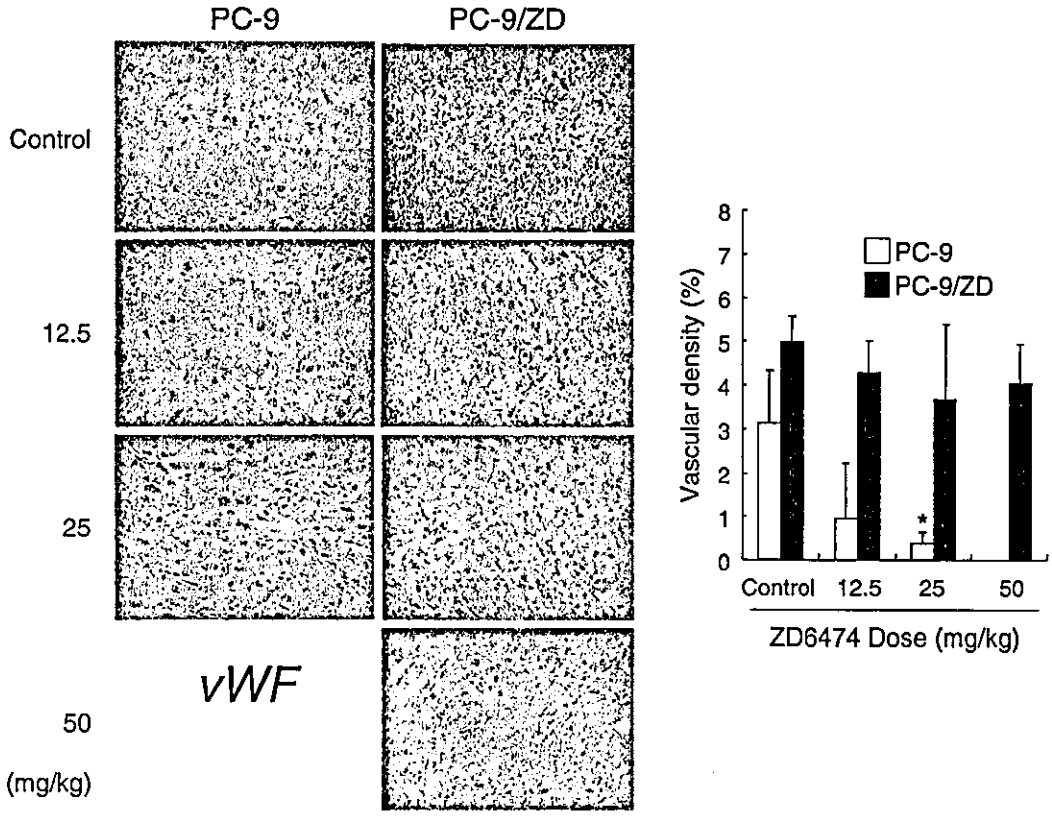

Fig. 5. Effect of ZD6474 on the vascular density of PC-9 and PC-9/ZD tumors stained *in vivo* with anti-vWF. Values are means±SD. Significant difference from the control by the Dunnett test (* $P<0.05$).

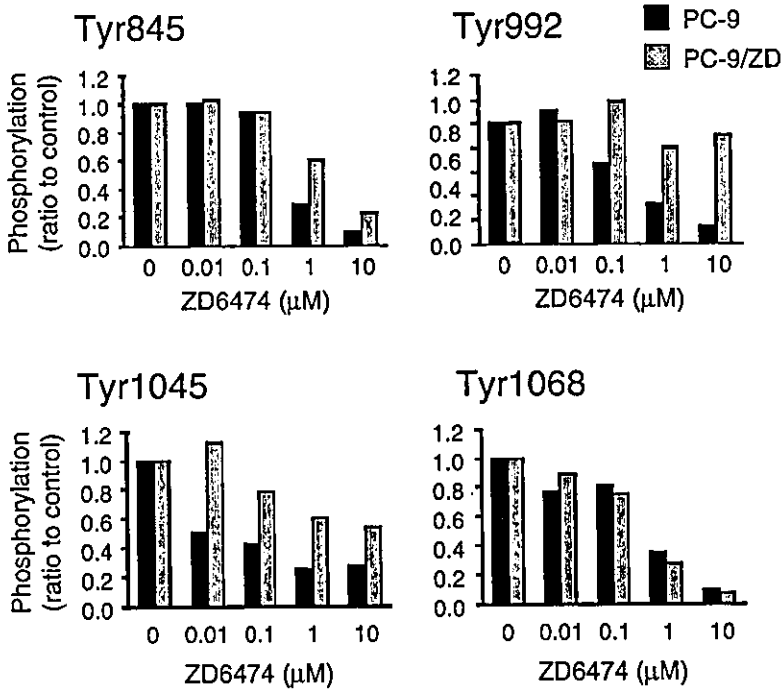

Fig. 6. Phosphorylation of EGFR tyrosine residues in PC-9 and PC-9/ZD cells after exposure to ZD6474.

phosphorylation in a dose-dependent manner. These results are consistent with previous reports[1] and indicate that ZD6474 is a potent EGFR TKI. *In vivo*, ZD6474 decreased vascular density in PC-9 tumors but not in PC-9/ZD cells, suggesting that ZD6474 may affect the angiogenic process via EGFR blockade. This could be mediated by inhibition of EGFR-induced paracrine production of angiogenic growth factors, such as VEGF, bFGF, and TGF from cancer cells, but the exact mechanism of action is unclear. This activity is, however, likely to be of less significance than the VEGFR-2-mediated antiangiogenic effect, since ZD6474 has been shown to have consistent *in vivo* antitumor activity in a range of histologically diverse human tumor xenografts, including activity in tumor models which do not respond to treatment with an EGFR TKI.[13] In addition, any change, or lack of change in microvessel density needs to be interpreted with caution as a either positive or negative indication of antiangiogenic activity, since the efficacy of antiangiogenic agents may not be related to microvessel density measurements.[14] ZD6474 was expected to induce increased apoptosis in tumor cells; although no induction of apoptosis was in fact observed, this may have been due to experimental factors.

Phosphorylations of Tyr845 and Tyr1045 of PC-9 and PC-9/ZD cells are similarly inhibited by ZD6474. On the other hand, while the inhibition pattern of Tyr845 phosphorylation by ZD6474 is coincident with that by gefitinib, the patterns at Tyr1045 are different. Therefore, we considered that the Tyr1045 is more important than Tyr845 for assessing the distinctive mode of action of ZD6474. In searching for a common mode of action of ZD6474 and gefitinib, Tyr845 seems to be the most promising site.

Phosphorylation of Tyr992 has been reported to transduce the signal to phospholipase C and protein kinase C.[15–17] In contrast, no inhibition of pan-phospho-PKC (the downstream signal of Tyr992) by gefitinib or ZD6474 was observed (data not shown). Tyr1045 has been reported to be linked to the Cbl-ubiquitin signaling pathway.[18] We have previously reported that Tyr1068 is a possible target site of EGFR for gefitinib[7], and gefitinib inhibited phosphorylation of Tyr1068 to varying degrees in PC-9 and PC-9/ZD cells, whereas ZD6474 inhibited Tyr1068 in both cell lines. These results suggest that the mode of inhibition of phosphorylation of EGFR by ZD6474 is subtly different to that of gefitinib. Therefore, although ZD6474 shows cross-resistance to gefitinib in these PC-9/ZD tumor cells, it has the potential for activity against gefitinib-resistant tumors through at least two mechanisms: (i) inhibition of EGFR-dependent downstream signaling pathways through differential effects on the phosphorylation status of tyrosine residues in the intracellular domain of EGFR, and (ii) inhibition of tumor angiogenesis through inhibition of VEGFR2 tyrosine kinase activity, which has not been examined in the present study. Site-directed mutagenesis studies are now under way to elucidate the biological significance of these sites.

1. Ciardiello F, Caputo R, Damiano V, Troiani T, Vitagliano D, Carlomagno F, Veneziani BM, Fontanini G, Bianco AR, Tortora G. Antitumor effects of ZD6474, a small molecule vascular endothelial growth factor receptor tyrosine kinase inhibitor, with additional activity against epidermal growth factor receptor tyrosine kinase. *Clin Cancer Res* 2003; 9: 1546–56.
2. Ciardiello F, Bianco R, Caputo R, Damiano V, Troiani T, Melisi D, De Vita F, De Placido S, Bianco AR, Tortora G. Antitumor activity of ZD6474, a vascular endothelial growth factor receptor tyrosine kinase inhibitor, in human cancer cells with acquired resistance to antiepidermal growth factor receptor therapy. *Clin Cancer Res* 2004; 10: 784–93.
3. Minami H, Ebi H, Tahara M, Sasaki Y, Yamamoto N, Yamada Y, Tamura T, Saijo N. A phase I study of an oral VEGF receptor tyrosine kinase inhibitor ZD6474, in Japanese patients with solid tumors. *Proc Am Soc Clin Oncol* 2003; 22: abstr 778.
4. Hurwitz H, Holden SN, Eckhardt SG, Rosenthal M, de Boer R, Rischin D, Green M, Basser R. Clinical evaluation of ZD6474, an orally active inhibitor of VEGF signaling, in patients with solid tumors. *Proc Am Soc Clin Oncol* 2002; 22: abstr 325.
5. Ciardiello F, Caputo R, Bianco R, Damiano V, Pomatico G, De Placido S, Bianco AR, Tortora G. Antitumor effect and potentiation of cytotoxic drugs activity in human cancer cells by ZD-1839 (Iressa), an epidermal growth factor receptor-selective tyrosine kinase inhibitor. *Clin Cancer Res* 2000; 6: 2053–63.
6. Moasser MM, Basso A, Averbuch SD, Rosen N. The tyrosine kinase inhibi-

tor ZD1839 ("Iressa") inhibits HER2-driven signaling and suppresses the growth of HER2-overexpressing tumor cells. *Cancer Res* 2001; **61**: 7184–8.
7. Koizumi F, Kanzawa F, Ueda Y, Koh Y, Tsukiyama S, Taguchi F, Tamura T, Saijo N, Nishio K. Synergistic interaction between the EGFR tyrosine kinase inhibitor gefitinib ("Iressa") and the DNA topoisomerase I inhibitor CPT-11 (irinotecan) in human colorectal cancer cells. *Int J Cancer* 2004; **108**: 464–72.
8. Koizumi F, Taguchi F, Shimoyama T, Saijo N, Nishio K. Mechanism of resistance to epidermal growth factor receptor inhibitor ZD1839: a role for inhibiting phosphorylation of EGFR at Tyr1068. *Am Assoc Cancer Res* 2003: abstr 1001.
9. Kawamura-Akiyama Y, Kusaba H, Kanzawa F, Tamura T, Saijo N, Nishio K, Arioka H, Ishida T, Fukumoto H, Kurokawa H, Sata M, Ohata M, Morikage T, Ohmori T, Fujiwara Y, Takeda Y. Non-cross resistance of ZD0473 in acquired cisplatin-resistant lung cancer cell lines. *Lung Cancer* 2002; **38**: 43–50.
10. Nishio K, Arioka H, Ishida T, Fukumoto H, Kurokawa H, Sata M, Ohata M, Saijo N, Morikage T, Ohmori T, Fujiwara Y, Takeda Y. Enhanced interaction between tubulin and microtubule-associated protein 2 via inhibition of MAP kinase and CDC2 kinase by paclitaxel. *Int J Cancer* 1995; **63**: 688–93.
11. Naruse I, Ohmori T, Ao Y, Fukumoto H, Kuroki T, Mori M, Saijo N, Nishio K. Antitumor activity of the selective epidermal growth factor receptor-tyrosine kinase inhibitor (EGFR-TKI) Iressa (ZD1839) in an EGFR-expressing multidrug-resistant cell line *in vitro* and *in vivo*. *Int J Cancer* 2002; **98**: 310–5.
12. Ono M, Hirata A, Kometani T, Miyagawa M, Ueda S, Kinoshita H, Fujii T, Kuwano M. Sensitivity to gefitinib (Iressa, ZD1839) in non-small cell lung cancer cell lines correlates with dependence on the epidermal growth factor (EGF) receptor/extracellular signal-regulated kinase 1/2 and EGF receptor/Akt pathway for proliferation. *Mol Cancer Ther* 2004; **3**: 465–72.
13. Wedge SR, Ogilvie DJ, Dukes M, Kendrew J, Chester R, Jackson JA, Boffey SJ, Valentine PJ, Curwen JO, Musgrove HL, Graham GA, Hughes GD, Thomas AP, Stokes ES, Curry B, Richmond GH, Wadsworth PF, Bigley AL, Hennequin LF. ZD6474 inhibits vascular endothelial growth factor signaling, angiogenesis, and tumor growth following oral administration. *Cancer Res* 2002; **62**: 4645–55.
14. Hlatky L, Hahnfeldt P, Folkman J. Clinical application of antiangiogenic therapy: microvessel density, what it does and doesn't tell us. *J Natl Cancer Inst* 2002; **94**: 883–93.
15. Holbrook MR, O'Donnell JB Jr, Slakey LL, Gross DJ, Bishayee A, Beguinot L, Bishayee S. Epidermal growth factor receptor internalization rate is regulated by negative charges near the SH2 binding site Tyr992. *Biochemistry* 1999; **38**: 9348–56.
16. Bishayee A, Beguinot L, Bishayee S. Phosphorylation of tyrosine 992, 1068, and 1086 is required for conformational change of the human epidermal growth factor receptor c-terminal tail. *Mol Biol Cell* 1999; **10**: 525–36.
17. Nogami M, Yamazaki M, Watanabe H, Okabayashi Y, Kido Y, Kasuga M, Sasaki T, Maehama T, Kanaho Y, Holbrook MR, O'Donnell JB Jr, Slakey LL, Gross DJ, Bishayee A, Beguinot L, Bishayee S. Requirement of autophosphorylated tyrosine 992 of EGF receptor and its docking protein phospholipase C gamma 1 for membrane ruffle formation. *FEBS Lett* 2003; **536**: 71–6.
18. Ravid T, Sweeney C, Gee P, Carraway KL 3rd, Goldkorn T. Epidermal growth factor receptor activation under oxidative stress fails to promote c-Cbl mediated down-regulation. *J Biol Chem* 2002; **277**: 31214–9.

Synergistic interaction between gefitinib (Iressa, ZD1839) and paclitaxel against human gastric carcinoma cells

Jong-Kook Park[a], Sang-Hak Lee[a], Jin-Hyoung Kang[b], Kazuto Nishio[c], Nagahiro Saijo[c] and Hyo-Jeong Kuh[a]

We have evaluated the antitumor effects of gefitinib (Iressa, ZD1839) in SNU-1 human gastric cancer cells (hMLH1-deficient and epidermal growth factor receptor-overexpressed) when given alone or as a doublet with oxaliplatin (LOHP), 5-fluorouracil (5-FU) or paclitaxel (PTX). The four drugs showed IC_{50}s ranging from 1.81 nM to 13.2 μM. LOHP and PTX induced G_2/M arrest, 5-FU increased S phase, and gefitinib increased G_1 in a concentration-dependent manner. The analysis using the previously developed cytostatic TP_I model showed that 64 and 80% of the overall growth inhibition was attributed to cell cycle arrest in cells exposed to 7.55 μM of LOHP or 10 nM of PTX for 72 h, respectively. PTX + gefitinib showed greatest synergism as determined by combination index analysis and apoptosis induced by PTX was potentiated by the co-administration of gefitinib. LOHP + gefitinib showed a similar, although to a lesser degree, synergistic effect. This study demonstrates the antitumor activity and the significant cell cycle arrest induced by gefitinib in SNU-1 human gastric carcinoma cells, and its synergistic interaction with LOHP and PTX. *Anti-Cancer Drugs* 15:809–818 © 2004 Lippincott Williams & Wilkins.

Anti-Cancer Drugs 2004, 15:809–818

Keywords: combination, gefitinib (ZD1839), human gastric carcinoma, oxaliplatin, paclitaxel

[a]Research Institute of New Drug Development, Catholic Research Institutes of Medical Science and [b]Division of Medical Oncology, The Catholic University of Korea, Seoul, South Korea and [c]Support Facility of Project Ward, National Cancer Center Hospital, Tokyo, Japan

Sponsorship: This work was supported in part by a grant from the Korea Health 21 R&D Project, Ministry of Health & Welfare (02-PJ2-PG1-CH12-0002), and by a grant from KOSEF (R04-2000-000-00052-0), Republic of Korea.

Correspondence to H.-J. Kuh, Catholic Research Institutes of Medical Science, Catholic University of Korea, 505 Banpo-dong, Seocho-ku, Seoul 137-401, South Korea.
Tel: +82 2 590 2422; fax: +82 2 592 2421;
e-mail: hkuh@catholic.ac.kr

Received 23 February 2004 Revised form accepted 4 June 2004

Introduction

The contemporary combination regimens for treatment of gastric cancer usually contain cisplatin and 5-fluorouracil (5-FU). Recently, the triplet combination of cisplatin, 5-FU and paclitaxel (PTX) has become one of the most highly active regimens against advanced gastric carcinoma [1].

Tumor tissues from gastric cancer patients show a high incidence of epidermal growth factor (EGF) and its receptor (EGFR) overexpression, both of which play a promotional role in the development of gastric cancer cooperatively with other members of the EGFR gene family, c-erbB-2 and c-erbB-3 [2]. The EGF and EGFR gene families have been associated with the growth regulation and gastric wall invasion in gastric cancers [3,4], and seem to be involved in determining the chemosensitivity of human cancer cells to chemotherapy [5]. Recently, it was also reported that inhibition of the EGFR cascade abrogated *Helicobacter pyroli*-induced up-regulation of vascular endothelial growth factor in gastric cancer cells [6]. A novel approach for the therapeutic blockade of EGFR signaling in human cancer has been recently developed based on the discovery of low-molecular-weight compounds that selectively inhibit the ligand-induced activation of EGFR tyrosine kinase (TK) and its receptor-mediated intracellular signaling [7]. Among various quinazoline-derived compounds tested as new anticancer drugs, gefitinib ([4-(3-chloro-4-fluoro-anilino)-7-methoxy-6-(3-morpholinopropoxy) quinazoline], also 'Iressa', ZD1839) has shown impressive preclinical activity in various tumor models *in vitro* and *in vivo* [7]. It is an orally active, selective EGFR-TK inhibitor that blocks the signal transduction pathways implicated in the proliferation and survival of cancer cells, and is currently under phase III clinical trial [7,8].

In addition, the methylation of DNA mismatch repair (MMR) genes has been observed in many human cancers, including gastric cancers. The methylation of the hMLH-1 promoter region has been shown to be involved in the mechanism of low or undetectable hMLH-1 protein expression in gastric tumors [9,10]. In addition to predisposing oncogenesis, the loss of MMR activity is related to drug resistance, since the MMR proteins play important roles in mediating the activation of cell cycle checkpoints and apoptosis in response to DNA damage induced by anticancer agents. This drug resistance extends to a variety of alkylating anticancer agents including platinum compounds, such as cisplatin and carboplatin [11]. Moreover, it has been shown that *N*-methyl-*N'*-nitro-*N*-nitrosoguanidine (MNNG)-resistant

0959-4973

human gastric cancer cells have very low or undetectable levels of hMLH-1 protein, which plays a key role with hMSH2 in the MMR system [12].

Oxaliplatin (LOHP) has a spectrum of activity that differs from that of cisplatin or carboplatin, suggesting that it has different molecular targets and/or different mechanism of resistance. It has been reported that MMR deficiencies do not induce similar resistance to LOHP [13], and because of this decreased possibility of resistance development, LOHP may serve as a good candidate for first-line treatment as a monotherapy or in combination with other agents in gastric cancer. Hence, LOHP may effectively substitute for cisplatin in the platinum-based triplet combination with 5-FU and PTX, as mentioned above.

In many studies, gefitinib in combination with radiation as well as a variety of cytotoxic agents, including taxanes and platinum compounds, has shown synergistic and supra-additive interactions in many types of cancers, such as colon, lung, breast, prostate and ovarian cancer [14]. However, no studies have been conducted on the antitumor effects of gefitinib given alone or in combination with cytotoxic agents against human gastric cancer cells.

In the present study, we evaluated the growth-inhibitory and cell cycle arrest effects of LOHP, 5-FU and PTX, which are promising cytotoxic drugs for the treatment of gastric carcinoma, and of a target-based cytostatic drug, gefitinib, in SNU-1 human gastric carcinoma cells that show MMR deficiency and EGFR overexpression. We also determined whether simultaneous EGFR blockade by gefitinib could improve the anticancer activities of these cytotoxic drugs. Our results show that the gefitinib + PTX combination had the greatest synergistic interaction. Gefitinib was found to potentiate the apoptosis induced by PTX.

Materials and methods

Chemicals

Clinical grade gefitinib and LOHP were kindly provided by AstraZeneca Pharmaceuticals (Macclesfield, UK) and Sanofi-Synthelabo (Malvern, PA), respectively. PTX and 5-FU were provided by the Drug Synthesis and Chemistry Branch, Developmental Therapeutics Program, Division of Cancer Treatment and Diagnosis, NCI (Bethesda, MD). Other drugs and reagents, unless otherwise stated, were purchased from Sigma (St Louis, MO).

Cell culture conditions

The human gastric cancer cell lines, SNU-1 and MKN-45, human lung adenocarcinoma cell line, A549, and human epidermoid carcinoma cell line, A431 were obtained from the Korean Cell Line Bank (Seoul, South Korea). Cells were maintained in RPMI 1640 supplemented with 10% heat-inactivated fetal bovine serum, 100 mg/ml of streptomycin and 100 U/ml penicillin in humidified air containing 5% (v/v) CO_2 at 37°C.

Western blotting

Total cell protein extracts were obtained as previously described [15]. Briefly, cells were lysed with lysis buffer [20 mM Tris–HCl (pH 7.5), 150 mM NaCl, 0.1% SDS, 1% Triton X-100, 1% sodium deoxycholate]. The lysate, containing 30 µg of total protein, was then mixed with 2 × SDS–PAGE sample buffer, boiled for 5 min and electrophoresed in 8% SDS gels under reducing conditions. The separated proteins were then electrophoretically transferred to PVDF membranes (Millipore, Bedford, MA) and the membranes were probed with a primary antibody against EGFR or hMLH1 (anti-human EGFR rabbit polyclonal antibody and anti-human hMLH1 rabbit polyclonal antibody; Santa Cruz Biotechnology, Santa Cruz, CA) at 1:1000 dilution. Immunoreactive proteins were detected by using an enhanced chemiluminescence detection system (Amersham Pharmacia Biotech, Little Chalfont, UK).

Measurement of growth inhibition

Growth inhibitory effects were measured by MTT assay and by direct cell counting [16]. For MTT assay, cells were plated in 96-well microtiter 24 h prior to treatment (4000 cells/well). Cells were exposed to various concentrations of the tested agents for 72 h. The absorbance of the reaction mixture was measured at 540 nm and the IC_{50} defined as the drug concentration required to reduce the absorbance to 50% of the control in each test was determined using an E_{max} model:

$$\%\ \text{Cell viability} = (100 - R) \times \left(1 - \frac{[D]^m}{K_d^m + [D]^m}\right) + R \quad (1)$$

where D is the drug concentration, K_d is the concentration of the drug that produces a 50% reduction in absorbance (i.e. IC_{50}), m is the Hill-type coefficient and R is the residual unaffected fraction (the resistant fraction). The Sigma Plot regression function was used for model fitting.

For direct cell counting, cells were seeded at a density of 1×10^6 in 100- or 150-mm Petri dishes at least 24 h prior to drug exposure and were exposed to two different concentrations of the drug for up to 72 h. The concentrations of each drug were 0.75 and 7.55 µM for LOHP, 9 and 65 µM for 5-FU, 2.5 and 10 nM for PTX, and 13 and 38 µM for gefitinib. At predetermined times, cells were harvested by resuspending then in PBS and then the total cell number was determined using a Counter (Coulter Electronics, Luton, UK). Trypan blue

exclusion under the microscope was used to determine the viable cell fraction. The remainder of the cell suspension samples was used for the cell cycle study (see below). For the combination study, gefitinib was given simultaneously with either LOHP, 5-FU or PTX for 72 h. Drugs were combined at equitoxic ratios (i.e. doses were applied in combinations that would have produced the same cytotoxic effect if the drugs were administered separately to produce a 50% growth inhibition, as determined by MTT assay). The cytotoxicities of the two-drug combinations were determined by MTT assay using the same procedure as used for single treatments. Each experiment was performed in triplicate.

Determination of combination effects

The cytotoxic effects obtained with two-drug combinations were analyzed using the Chou and Talalay method [17]. The interaction between two drugs was assessed by using combination index (CI) (2). CI was calculated for a cell death range of 20–80 %, i.e. CI_{20}–CI_{80}.

$$CI_x = \frac{(D)_A}{(D_x)_A} + \frac{(D)_B}{(D_x)_B} + \alpha \cdot \frac{(D)_A(D)_B}{(D_x)_A(D_x)_B} \qquad (2)$$

where CI_x is the CI for a fixed effect, x [fraction affected (f_a)·100], for a combination of drug A and drug B, $(D_x)_A$ is the concentration of drug A alone giving an effect x, $(D_x)_B$ is the concentration of drug B alone giving an effect x, $(D)_A$ is the concentration of drug A in combination A + B giving an effect x, $(D)_B$ is the concentration of drug B in combination A + B giving an effect x, and α is a parameter with value 0 when A and B are mutually exclusive and 1 when A and B are mutually non-exclusive. A CI_x between 0.8 and 1.2 was categorized as additive, less than 0.8 as synergistic, and greater than 1.2 as antagonistic.

Measurement of cell cycle effect

Cells were plated and treated as described above (see measurement of growth inhibition by direct cell counting). For the combination of PTX and gefitinib, cells were exposed to 1.25 nM of PTX and 8.5 μM of gefitinib or 0.6 nM of PTX and 4 μM of gefitinib. After harvesting, the cells were fixed in 10 ml of 70% cold ethanol while vortexing, and cells were kept at 4°C for 1 h and stored at –20°C until analysis. Upon analysis, fixed cells were washed and resuspended in 1 ml of PBS containing 50 μg/ml RNase A and 50 μg/ml propidium iodide. After 20 min incubation at 37°C, cells were analyzed for DNA content by flow cytometry (FACSVantage; Becton Dickinson Immunocytometry Systems, San Jose, CA). For each sample, 10 000 events were acquired. Cell cycle distribution was determined using cell cycle analysis software (Modfit; Verity, Topsham, ME).

Cytostatic model analysis

In order to predict the contribution of cell cycle arrest to the overall growth inhibition induced by a cytotoxic agent, we used the cytostatic TP_i model as described previously [18]. In brief, the model assumptions were: (1) exponential growth of a cell population with a growth rate constant (k); (2) all cells were in cycle, i.e. no cell deaths and no G_0 phase arrest; (3) that the distribution of cell numbers in a cell cycle follows the age structure of a simple exponential population. $TP_i(t)$, the transition probability for i phase at time t, was defined as $(\alpha_i(t)-\alpha_i(t+\Delta t))/\alpha_i(t)/\Delta t$, where $\alpha_i(t) = [N_i(t)-(\#$ cells already exiting from i phase at time $t)]/N_i(t)$ and $N_i(t)$ is the number of cells in i phase at time t. The transition probability for each cell cycle check point, i.e. $TP_{G1}(t)$, $TP_S(t)$ and $TP_{G2/M}(t)$, was calculated using $F_i(t)$, the fraction of cells in the G_1, S and G_2/M phases at time t, and $k(t)$, the growth rate constant. The simulation of cell population growth over time was performed using a numerical method based on the cell population growth algorithm using $TP_i(t)$ and $F_i(t)$. This model assumes no cell death during cell cycle progression; hence, the simulation result represents a reduction in the number of cells resulting from cell cycle arrest (or disturbed cell cycle progression) only. The model should underestimate growth inhibition in the presence of cell death and the difference between the model-predicted and the observed growth curve of a treated cell population represents the growth inhibition resulting from cell death in the population.

Simultaneous measurement of drug-induced apoptosis and cell cycle distribution

For simultaneous determination of cell cycle contents and apoptosis, the user's manual of Apo-Direct kit (PharMingen, San Diego, CA) was followed. Briefly, after harvest, cells were fixed in 1% paraformaldehyde/PBS on ice for 15 min and resuspended in 70% ice-cold ethanol. Cells were then incubated in 50 μg of solution containing terminal deoxynucleotidyltransferase and FITC-conjugated dUTP deoxynucleotides 1:1 in reaction buffer for 2 h at 37°C in the dark. After washing in PBS containing 0.1% Triton X-100, the cells were stained with 5 μg of propidium iodide and 10 kU of RNase in 1 ml of PBS for 20 min at 37°C. Flow cytometric analysis was performed with FL1 (FITC) and FL2 (propidium iodide) and data acquisition and analysis were done using CellQuest software (Becton Dickinson Immunocytometry Systems).

Statistical analysis

Statistical comparisons were completed using Student's paired t-test; $p < 0.05$ was considered statistically significant.

Results

hMLH-1 and EGFR expression in SNU-1 and MKN45

We evaluated the antitumor activities of the three cytotoxic drugs, LOHP, 5-FU or PTX, and that of a cytostatic drug, gefitinib, alone and in doublet combinations. We selected SNU-1 human gastric carcinoma cells because they are known to be MMR deficient due to a

missense mutation in hMLH-1 [12], which was confirmed in this study (Fig. 1A). EGFR expression was also examined and significant expression was observed in these cells. The level of expression was higher than those in MKN-45, another human gastric cancer cell line, and in A549, a human lung cancer cell line (Fig. 1B and 1C). Hence, SNU-1 cells were considered to represent an *in vitro* gastric cancer model that may have intrinsic chemoresistance related to both MMR deficiency and EGFR overexpression.

Cytotoxicity of LOHP, 5-FU, PTX and gefitinib in SNU-1 cells

Dose–response curves were analyzed using an E_{max} model with a resistant fraction (R), which represents the fraction of cells insensitive to the drug (Table 1). Significant R values were obtained for PTX (mean of 32%), whereas the other three drugs showed a full dose–response curve with percentage cell viabilities decreasing almost to the base line level (< 10%). The IC_{50} showed a wide range from 1.81 nM to 13.2 μM, i.e. 0.788 μM for LOHP, 9.35 μM for 5-FU, 1.81 nM for PTX and 13.2 μM for gefitinib. The antiproliferative activity of these agents was confirmed by direct cell counting. Drugs were given at two different concentrations, i.e. at the IC_{50} and IC_{80} levels. For all agents, 72 h exposure exhibited 50–60 and 80–90% growth inhibition at the IC_{50} and IC_{80} drug concentrations, respectively (Fig. 2). For PTX, 10 nM induced 68% growth inhibition when measured by MTT assay, with no further inhibition at higher concentrations, nonetheless, 89% inhibition was observed by direct cell counting (Fig. 2C).

Fig. 1

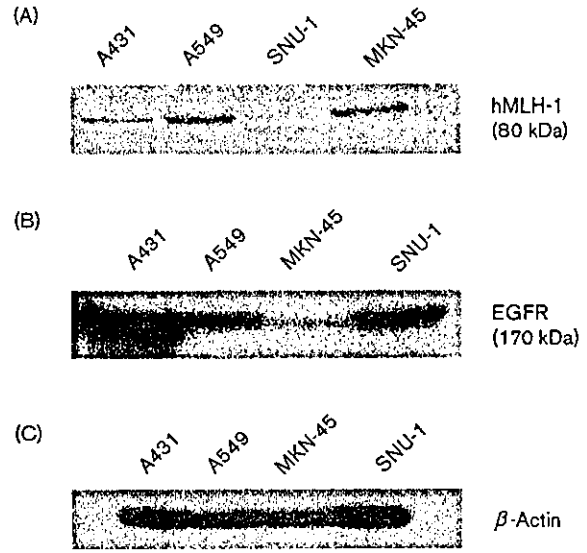

Western blot analysis of hMLH-1 (A) and EGFR (B) expression in A549, A431, SNU-1 and MKN-45 cells. The relative expression levels of EGFR relative to β-actin (C) were compared for these four cell lines.

Cytostatic model analysis

Growth inhibition, i.e. the reduction in the growth rate of a cell population following drug treatment, is the result of cell cycle arrest (cytostatic effect) and cell death (cytotoxic effect). As previously reported, we have developed a computational model (a cytostatic model, because the model assumes no cell death to predict the growth inhibition resulting from cell cycle arrest only) to assess the respective contributions of cell cycle arrest and cell death to the overall growth inhibition induced by cytotoxic anticancer agents [18]. We used this cytostatic model to analyze the contribution of cell cycle arrest to overall growth inhibition when SNU-1 cells were treated with each cytotoxic agent. The time course of cell cycle distribution was determined in SNU-1 cells exposed to LOHP, 5-FU and PTX at IC_{80} levels, respectively, and used in model simulation (part of data shown in Fig. 3). Since the model uses the percentage of cells in each phase to simulate the growth of a cell population, predictions cannot be made with 0% in any phase at anytime. For this reason, this cytostatic model was used only for LOHP and PTX, but not for 5-FU, because in this case the percentage of cells in the G_2/M phase was zero after 12 h exposure (data not shown). The cytostatic computational model predicted 64% of the overall inhibition from the cell cycle arrest induced by LOHP after 72 h exposure at 7.55 μM. For PTX given for 72 h at 10 nM and 80% of the overall inhibition was attributed to cell cycle arrest by the model. These results indicate that the reduction in population growth rate caused by cell

Table 1 Parameters of the antiproliferative activities of LOHP, 5-FU, PTX and gefitinib against SNU-1 human gastric carcinoma cells

	LOHP	5-FU	PTX	Gefitinib
IC_{50}[a]	0.788 ± 0.142	9.35 ± 1.57	1.81 ± 0.67	13.2 ± 0.33
R[b]	5.00 ± 4.48	8.53 ± 7.64	32.0 ± 11.1	0
m[c]	0.811 ± 0.135	0.793 ± 0.125	5.02 ± 0.80	1.14 ± 0.10

Each value represents mean ± SD of three independent experiments.
[a]IC_{50} is the concentration of the drug that kills 50% of cancer cells compared to the control after 72 h of continuous exposure. Expressed in μM, except for paclitaxel, which is in nM.
[b]R is the residual unaffected fraction (resistance fraction) (1) and is equal to $(100 - E_{max})$.
[c]m is the Hill-type coefficient (1).

Fig. 3

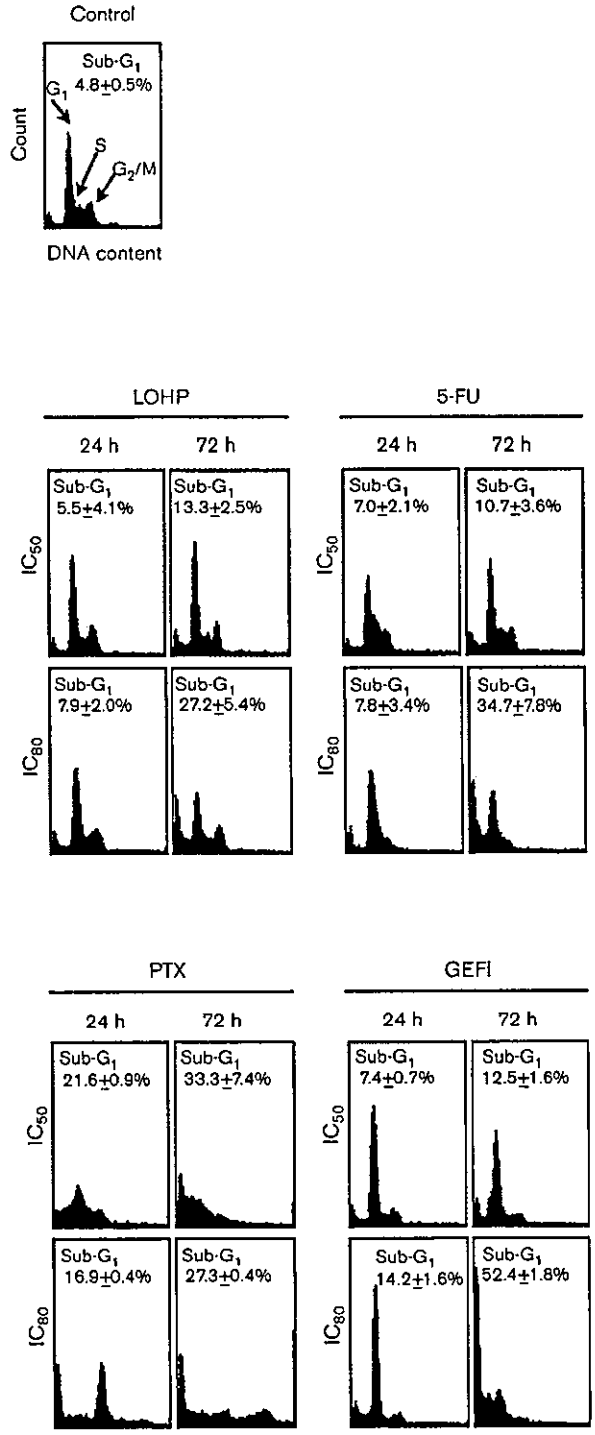

DNA histogram analysis in cells exposed to LOHP, 5-FU, PTX and gefitinib (GEFI) single treatment at IC_{50} and IC_{80}. Representative histograms are shown for 24 and 72 h post-treatment with the percentage of cells in sub-G_1 phase. Cells were harvested and fixed with ethanol before treated with RNase. Cells were then stained with propidium iodide and analyzed by flow cytometry. The concentrations were: 0.75 and 7.55 μM for LOHP, 9 and 65 μM for 5-FU, 2.5 and 10 nM for PTX, and 13 and 38 μM for GEFI.

additive. 5-FU + gefitinib was found additive with CI values ranging from 1.06 to 1.24. The combination of PTX + gefitinib showed greatest synergism: with CI values of less than 1.0 (0.28–0.99) for the whole f_a range; in particular, the resistant fraction associated with PTX single treatment was abrogated when combined with gefitinib, indicating a greater advantage compared to the other combinations (Fig. 4). For PTX + gefitinib, the most synergistic combination, the cell cycle arrest and apoptosis induction were studied in cells exposed to the simultaneous treatment of PTX and gefitinib at two different concentrations, i.e. 0.62 nM PTX + 4 μM gefitinib (combination IC_{50}) and 1.25 nM PTX + 8.5 μM gefitinib (combination IC_{65}) (Fig. 6). No significant changes in the cell cycle distribution were observed at the combination IC_{50} level until 72 h. At the higher concentration, i.e. 1.25 nM PTX + 8.5 μM gefitinib (around IC_{65}), a significant decrease in G_1 phase cells occurred with rapid increase in sub-G_1 cells. The simultaneous staining of DNA content and DNA strand breaks were used to discern the apoptotic cells as well as necrotic cells from viable cells (Fig. 6). The combination of PTX and gefitinib at the IC_{50} and IC_{65} level induced 100 and 35% increase ($p < 0.05$) in apoptosis (TUNEL-positive cells), respectively, compared to the single treatment, supporting the synergism between these two drugs.

Discussion

Systemic chemotherapy for the treatment of gastric carcinomas includes mitomycin C, anthracyclines, alkylating agents and 5-FU. Among these drugs, cisplatin and 5-FU are most commonly used in combination regimens. Recently, PTX has been added and a triplet combination of PTX, 5-FU and cisplatin has also been evaluated for the treatment of advanced gastric cancer [20]. In addition, a new platinum compound, LOHP, may replace cisplatin due to its reduced toxicity and decreased possibility of resistance development related to MMR deficiency. Hence, we undertook to evaluate in human gastric cancer cells the antitumor activities of LOHP, 5-FU and PTX, and the potential synergistic interactions between these cytotoxic agents individually and a newly developed target-based (cytostatic) drug, gefitinib, to provide preclinical data for the future clinical development of these agents in a combination setting for the treatment of advanced gastric carcinomas.

The *in vitro* antitumor activity of the four agents was evaluated by MTT assay. SNU-1 cells showed differential sensitivity toward these agents, and the rank order of sensitivities was PTX (1.81 nM) > LOHP (0.788 μM) > 5-FU (9.35 μM) > gefitinib (13.2 μM). Among these four agents, PTX showed the greatest cytotoxicity with an IC_{50} in the nanomolar range; however a significant

Fig. 4

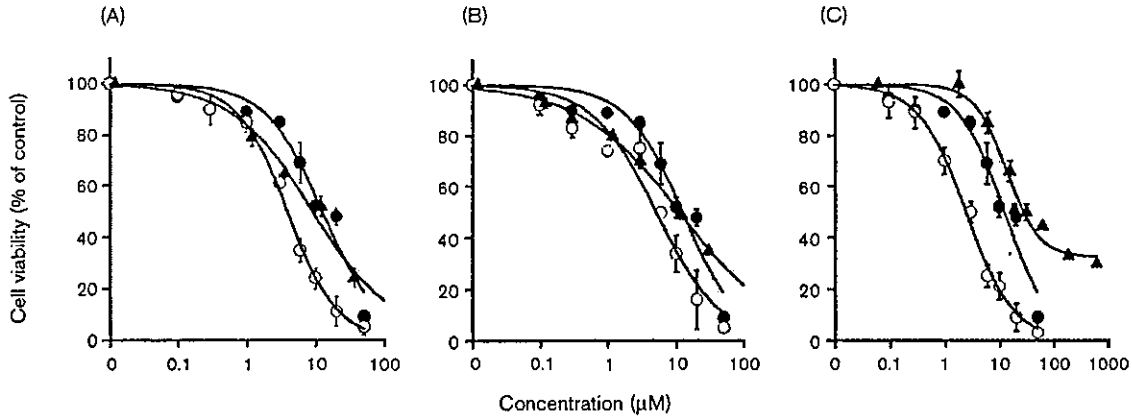

Representative dose–response curves of LOHP, 5-FU, PTX and gefitinib administered alone and in combination. (A) Gefitinib alone (solid circles), LOHP alone (solid triangles), LOHP + gefitinib (open circles); (B) gefitinib alone (solid circles), 5-FU alone (solid triangles), 5-FU + gefitinib (open circles); and (C) gefitinib alone (solid circles), PTX alone (solid triangles), PTX + gefitinib (open circles). Cells were simultaneously exposed to each treatment regimen for 72 h and cell viability was determined by MTT assay. The *x*-axis is [gefitinib] × 1, [LOHP] × 12, [5–FU] × 1.2 and [PTX] × 6250.

fraction of resistant cells was found (Table 1). Such PTX-resistant fractions have been observed in other cell lines, such as A549, a human lung adenocarcinoma cell line, and in FaDu, a pharynx squamous carcinoma cell line, when cell viability was measured by the MTT or the SRB assay (unpublished data). In the case of PTX, the growth-inhibitory effect as measured by two different methods produced different results, i.e. MTT versus direct cell counting (Table 1 and Fig. 2). The exposure of cells to 10 nM of PTX for 72 h induced around 90% growth inhibition, when determined by direct cell counting, whereas 68% growth inhibition was expected based on MTT data. In the cases of the other three agents, the MTT data agreed with direct cell counting. Therefore, the resistant fraction obtained in the MTT assay seemed to be associated with the assay method, especially for PTX, suggesting that the experimental data obtained by widely used viability assays, such as MTT and SRB, should be interpreted with caution when determining the cytotoxicity of PTX in monolayer cultures. However, in the present study, this did not affect the degree of synergy calculated for gefitinib + PTX since the maximum concentration of PTX used for the CI calculation was 2.5 nM, where no difference was observed between the cell counting and MTT results (Fig. 2).

SNU-1 cells showed significant resistance to 5-FU, i.e. the IC_{50} of 5-FU in SNU-1 cells was rather high (9.35 μM), which is close to that of gefitinib, a known cytostatic drug. MMR-proficient MKN-45 cells showed about 3 times higher sensitivity to 5-FU than SNU-1 cells (unpublished data). Hence, this intrinsic resistance of SNU-1 to 5-FU may be related to its MMR deficiency [15].

Fig. 5

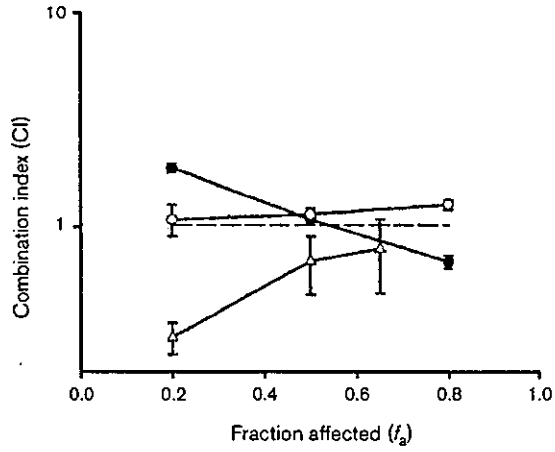

Combination index (CI_x) versus affected fraction (f_a) plots for LOHP + gefitinib (solid circles), 5-FU + gefitinib (open circles) and PTX + gefitinib (open squares) in SNU-1 cells. Cells were treated with LOHP or 5-FU or PTX + gefitinib at fixed equitoxic ratios. CI < 0.8, CI = 1 and CI > 1.2 indicate synergism, additivity and antagonism, respectively. LOHP and gefitinib were treated at a 0.083:1 molar ratio, 5-FU and gefitinib at 0.83:1, and PTX and gefitinib at 0.00016:1. CI_x was calculated using E_{max} model parameters obtained from the MTT data shown in Fig. 4.

It has been suggested that the inhibition of EGFR-TK is an effective antiproliferative principle in EGFR-positive human gastric cancer cells [4]. Recently, gefitinib showed antiangiogenic and antiproliferative activity in a variety of human cancer cells *in vitro*, including human gastric cancer cells (KATO III and N87) [21]. The cytostatic growth inhibitory activity of gefitinib has been